Supplemental Data

A

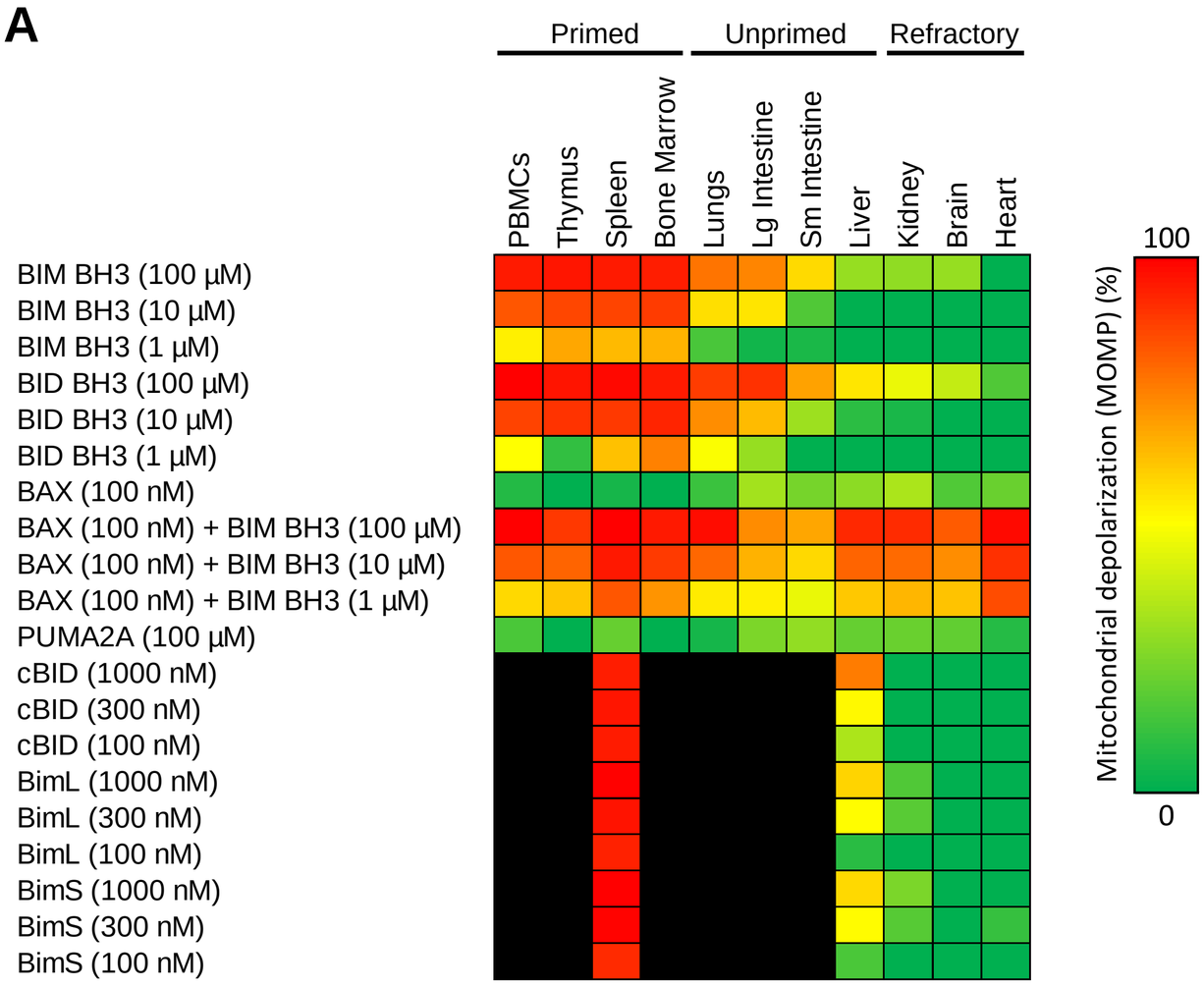

B

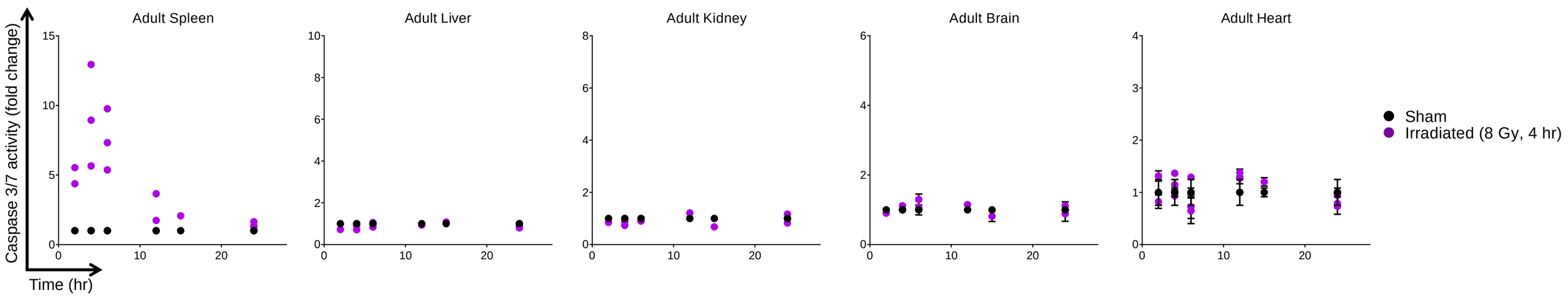

C

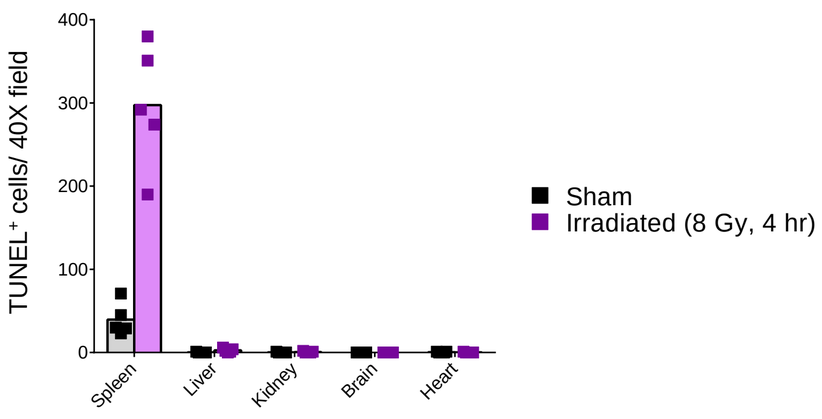

Figure S1: Measuring apoptotic priming with full-length proteins across adult mouse tissues (Related to Figure 1). (A) Summary BH3 Profiling data across healthy adult mouse tissues. Data were compiled from three indepenadent experiments. (B) Mice were irradiated and tissues were collected at the indicated time points and caspase 3/7 activity was measured. Data shown are mean ± SD, 2 independent experiments (IEs). (C) Mice were irradiated and tissues were collected after four hours and processed for TUNEL staining. Each point represents the total TUNEL$^+$ cells counted within a 40X field of view (FOV) in each tissue in one experiment. Bars represent means.

Table S1: Peptide-level mass spectrometry data for human protein expression (Related to Figure 1).

Protein	Peptide	Length	Protein Accessio	Gene Symbol	Genespecific	IsoformSpecif	Shared
	GGGPTSSEQIMK	12	gi|242117893|re	BAX	True	False	True
	IGDELDSNMELQR	13	gi|242117893|re	BAX	True	False	True
	KLSECLK	7	gi|242117893|re	BAX	True	False	True
	KLSECLKR	8	gi|242117893|re	BAX	True	False	True
	LLKPPHPHHR	10	gi|4757838|ref|	BAX	True	True	False
	LSECLK	6	gi|242117893|re	BAX	True	False	True
	LSECLKR	7	gi|242117893|re	BAX	True	False	True
	MDGSGEQPRGGGPTSSEQIMK	21	gi|242117893|re	BAX	True	False	True
	MDGSGEQPR	9	gi|242117893|re	BAX	True	False	True
BAX	MGGEAPELALDPVPQDASTK	20	gi|242117893|re	BAX	True	False	True
	MGGEAPELALDPVPQDASTKK	21	gi|242117893|re	BAX	True	False	True
	MIAAVDTDSPREVFFR	16	gi|242117893|re	BAX	True	False	True
	MIAAVDTDSPR	11	gi|242117893|re	BAX	True	False	True
	RIGDELDSNMELQR	14	gi|242117893|re	BAX	True	False	True
	TGALLLQGFIQDR	13	gi|242117893|re	BAX	True	False	True
	TIMGWTLDFLR	11	gi|242117893|re	BAX	True	False	True
	VAADMFSDGNFNWGR	15	gi|242117893|re	BAX	True	False	True
	VVALFYFASK	10	gi|242117893|re	BAX	True	False	True
	VPELIR	6	gi|4502053|ref|	ALOX12B;BAX;CLIP4	False	False	True
BAK	ASGQGPGPPR	10	gi|4502363|ref|	BAK1	True	True	False
	FVVDFMLHHCIAR	13	gi|4502363|ref|	BAK1	True	True	False
	HQQEQEAEGVAAPADPEMVTLPLQPSSTMGQ	34	gi|4502363|ref|	BAK1	True	True	False
	IATSLFESGINWGR	14	gi|4502363|ref|	BAK1	True	True	False
	LALHVYQHGLTGFLGQVTR	19	gi|4502363|ref|	BAK1	True	True	False
	MASGQGPGPPR	11	gi|4502363|ref|	BAK1	True	True	False
	QECGEPALPSASEEQVAQDTEEVFR	25	gi|4502363|ref|	BAK1	True	True	False
	QLAIIGDDINR	11	gi|4502363|ref|	BAK1	True	True	False
	QLAIIGDDINRR	12	gi|4502363|ref|	BAK1	True	True	False
	SYVFYR	6	gi|4502363|ref|	BAK1	True	True	False
	VVALLGFGYR	10	gi|4502363|ref|	BAK1	True	True	False
	YDSEFQTMLQHLQPTAENAYEYFTK	25	gi|4502363|ref|	BAK1	True	True	False
	DFAEMSSQLHLTPFTAR	17	gi|72198189|ref	BCL2	True	False	True
	FATVVEELFR	10	gi|72198189|ref	BCL2	True	False	True
BCL-2	GYEWDAGDVGAAPPGAAPAPGIFSSQPGHTP	42	gi|72198189|ref	BCL2	True	False	True
	GYEWDAGDVGAAPPGAAPAPGIFSSQPGHTP	37	gi|72198189|ref	BCL2	True	False	True
	QAGDDFSR	8	gi|72198189|ref	BCL2	True	False	True
	TSPLQTPAAPGAAAGPALSPVPPVVHLTLR	30	gi|72198189|ref	BCL2	True	False	True
	AFSDLTSQLHITPGTAYQSFEQVVNELFR	29	gi|20336335|ref	BCL2L1	True	True	False
	EAGDEFELR	9	gi|4502381|ref|	BCL2L1	True	False	True
	ELVVDFLSYK	10	gi|4502381|ref|	BCL2L1	True	False	True
BCL-XL	EMQVLVSR	8	gi|20336335|ref	BCL2L1	True	True	False
	EVIPMAAVK	9	gi|4502381|ref|	BCL2L1	True	False	True
	GYSWSQFSDVEENR	14	gi|4502381|ref|	BCL2L1	True	False	True
	QALREAGDEFELR	13	gi|4502381|ref|	BCL2L1	True	False	True
BCL-2/BCL-XL	DGVNWGR	7	gi|72198189|ref	BCL2L1;BCL2	False	False	True
	LLFFAPTR	8	gi|11386165|ref	MCL1	True	False	True
	NHETAFQGMLR	11	gi|11386165|ref	MCL1	True	False	True
	TINQESCIEPLAESITDVLVR	21	gi|11386165|ref	MCL1	True	False	True
MCL-1	VARPPPIGAEVPDVTATPAR	20	gi|11386165|ref	MCL1	True	False	True
	KALETLR	7	gi|19924129|ref	MCL1;RAD50	False	False	True
	ALETLR	6	gi|54792138|ref	RAD50;MCL1;HELZ	False	False	True
	IGDEFNAYYAR	11	gi|5729740|ref|	BCL2L11	True	False	True
	QAEPADMRPEIWIAQELR	18	gi|5729740|ref|	BCL2L11	True	False	True
BIM	QLQPAERPPQLRPGAPTSLQTEPQDRSPAPMSG	63	gi|323362973|re	BCL2L11	True	True	False
	QPSDVSSECDR	11	gi|5729740|ref|	BCL2L11	True	False	True
	VFLNNYQAAEDHPR	14	gi|5729740|ref|	BCL2L11	True	False	True
	DLATALEQLLQAYPRDMEKEK	21	gi|347300410|re	BID	True	False	True
	DLATALEQLLQAYPR	15	gi|347300410|re	BID	True	False	True
	DVFHTTVNFINQNLR	15	gi|347300410|re	BID	True	False	True
	ELDALGHELPVLAPQWEGYDELQTDGNR	28	gi|347300410|re	BID	True	False	True
	HLAQVGDSMDR	11	gi|347300410|re	BID	True	False	True
	IEADSESQEDIIR	13	gi|347300410|re	BID	True	False	True
BID	KVASHTPSLLR	11	gi|347300410|re	BID	True	False	True
	LGRIEADSESQEDIIR	16	gi|347300410|re	BID	True	False	True
	RELDALGHELPVLAPQWEGYDELQTDGNR	29	gi|347300410|re	BID	True	False	True
	SIPPGLVNGLALQLR	15	gi|347300410|re	BID	True	False	True
	TMLVLALLLAK	11	gi|347300410|re	BID	True	False	True
	VASHTPSLLR	10	gi|347300410|re	BID	True	False	True

Protein	Peptide	Length	Protein Accessio	Gene Symbol	Genespecific	IsoformSpecif	Shared
	DGSWFIQSLCAMLK	14	gi|14790119|ref	CASP3	True	False	True
	EEIVELMR	8	gi|14790119|ref	CASP3	True	False	True
	ELYFYH	6	gi|14790119|ref	CASP3	True	False	True
	GTELDCGIETDSGVDDDMACHK	22	gi|14790119|ref	CASP3	True	False	True
	GTELDCGIETDSGVDDDMACHKIPVEADFLYAY	43	gi|14790119|ref	CASP3	True	False	True
	IIHGSESMDSGISLDNSYK	19	gi|14790119|ref	CASP3	True	False	True
	IPVEADFLYAYSTAPGYYSWR	21	gi|14790119|ref	CASP3	True	False	True
	ITNFFR	6	gi|14790119|ref	CASP3	True	False	True
	KITNFFR	7	gi|14790119|ref	CASP3	True	False	True
	LEFMHILTR	9	gi|14790119|ref	CASP3	True	False	True
	LFIIQACR	8	gi|14790119|ref	CASP3	True	False	True
Caspase 3	MDYPEMGLCIIINNK	15	gi|14790119|ref	CASP3	True	False	True
	MENTENSVDSK	11	gi|14790119|ref	CASP3	True	False	True
	NKNDLTREEIVELMR	15	gi|14790119|ref	CASP3	True	False	True
	NKNDLTR	7	gi|14790119|ref	CASP3	True	False	True
	NLKYEVR	7	gi|14790119|ref	CASP3	True	False	True
	QIPCIVSMLTK	11	gi|14790119|ref	CASP3	True	False	True
	QYADKLEFMHILTR	14	gi|14790119|ref	CASP3	True	False	True
	SGTDVDAANLR	11	gi|14790119|ref	CASP3	True	False	True
	SLTGKPK	7	gi|14790119|ref	CASP3	True	False	True
	SSFVCVLLSHGEEGIIFGTNGPVDLKK	27	gi|14790119|ref	CASP3	True	False	True
	STGMTSR	7	gi|14790119|ref	CASP3	True	False	True
	VATEFESFSFDATFHAK	17	gi|14790119|ref	CASP3	True	False	True
	AGFLYTGEGDTVR	13	gi|32528299|ref	XIAP	True	False	True
	AGFYALGEGDKVK	13	gi|32528299|ref	XIAP	True	False	True
	DHFALDRPSETHADYLLR	18	gi|32528299|ref	XIAP	True	False	True
	DSMQDESSQTSLQK	14	gi|32528299|ref	XIAP	True	False	True
	EEEFVEEFNR	10	gi|32528299|ref	XIAP	True	False	True
	EISTEEQLR	9	gi|32528299|ref	XIAP	True	False	True
	GQEYINNIHLTHSLEECLVR	20	gi|32528299|ref	XIAP	True	False	True
	IQISGSNYK	9	gi|32528299|ref	XIAP	True	False	True
	NPAMYSEEAR	10	gi|32528299|ref	XIAP	True	False	True
	NPSMADYEAR	10	gi|32528299|ref	XIAP	True	False	True
XIAP	SESDAVSSDR	10	gi|32528299|ref	XIAP	True	False	True
	SFQNWPDYAHLTPR	14	gi|32528299|ref	XIAP	True	False	True
	SLEVLVADLVNAQK	14	gi|32528299|ref	XIAP	True	False	True
	TCVPADINKEEEFVEEFNR	19	gi|32528299|ref	XIAP	True	False	True
	TCVPADINKEEEFVEEFNRLK	21	gi|32528299|ref	XIAP	True	False	True
	TFANFPSGSPVSASTLAR	18	gi|32528299|ref	XIAP	True	False	True
	TGQVVDISDTIYPR	14	gi|32528299|ref	XIAP	True	False	True
	TPSLTR	6	gi|32528299|ref	XIAP	True	False	True
	VENYLGSR	8	gi|32528299|ref	XIAP	True	False	True
	WQYGDSAVGR	10	gi|32528299|ref	XIAP	True	False	True
	HILDEK	6	gi|22749293|ref	FANCB;APAF1	False	False	True
	SVMGPK	6	gi|7108333|ref|	HDLBP;APAF1	False	False	True
	GHLLGR	6	gi|13994259|ref	AF5;RPL13A;MRPS5;AGPS;A	False	False	True
	FSPDDK	6	gi|8922301|ref|	VDR70;FER1L5;APAF1;NOP1	False	False	True
	ADLPEQAHSIIK	12	gi|7108333|ref|	APAF1	True	False	True
	AFDSQCQILLTTR	13	gi|7108333|ref|	APAF1	True	False	True
	AHEDEVLCCAFSTDDR	16	gi|7108333|ref|	APAF1	True	False	True
	DFVCHQGTVLSCDISHDATK	20	gi|7108333|ref|	APAF1	True	False	True
	DKSVTDSVMGPK	12	gi|7108333|ref|	APAF1	True	False	True
	DLAALLHDGIPVVSSSSGK	19	gi|32483359|ref	APAF1	True	False	True
	DNDSYVSFYNALLHEGYK	18	gi|7108333|ref|	APAF1	True	False	True
	DSVSGITSYVR	11	gi|32483359|ref	APAF1	True	False	True
	DYYTDLSILQK	11	gi|7108333|ref|	APAF1	True	False	True
	ECKVVER	7	gi|32483363|ref	APAF1	True	True	False
	EDIKDYYTDLSILQK	15	gi|7108333|ref|	APAF1	True	False	True
	FIATCSVDK	9	gi|7108333|ref|	APAF1	True	False	True
	FIATCSVDKK	10	gi|7108333|ref|	APAF1	True	False	True
	GHQETVKDFR	10	gi|7108333|ref|	APAF1	True	False	True
	GSPLVVSLIGALLR	14	gi|7108333|ref|	APAF1	True	False	True
	HILDEKDCAVSENFQEFLSLNGHLLGR	27	gi|7108333|ref|	APAF1	True	False	True
	IHVSPDFK	8	gi|7108333|ref|	APAF1	True	False	True
	IITQFQR	7	gi|7108333|ref|	APAF1	True	False	True
	IWSFDLLLPLHELR	14	gi|7108333|ref|	APAF1	True	False	True
	KADLPEQAHSIIK	13	gi|7108333|ref|	APAF1	True	False	True
	KIHVSPDFK	9	gi|7108333|ref|	APAF1	True	False	True
	KLVNAIQQK	9	gi|7108333|ref|	APAF1	True	False	True
	LDQDESFSQR	10	gi|7108333|ref|	APAF1	True	False	True
APAF-1	LLASCSADGTLK	12	gi|7108333|ref|	APAF1	True	False	True
	LLSWSFDGTVK	11	gi|7108333|ref|	APAF1	True	False	True
	LPLNIEEAKDR	11	gi|7108333|ref|	APAF1	True	False	True
	LPLNIEEAK	9	gi|7108333|ref|	APAF1	True	False	True
	LQNLCTR	7	gi|7108333|ref|	APAF1	True	False	True
	LVNAIQQK	8	gi|7108333|ref|	APAF1	True	False	True
	LVVRPHTDAVYHACFSEDGQR	21	gi|7108333|ref|	APAF1	True	False	True
	LWDATSANER	10	gi|7108333|ref|	APAF1	True	False	True
	LWDLNQK	7	gi|7108333|ref|	APAF1	True	False	True
	NCLLQHR	7	gi|7108333|ref|	APAF1	True	False	True
	NCSQLQDLHK	10	gi|7108333|ref|	APAF1	True	False	True
	NEPTQQQR	8	gi|7108333|ref|	APAF1	True	False	True
	NITNLSR	7	gi|7108333|ref|	APAF1	True	False	True
	NTMFGHTNSVNHCR	14	gi|7108333|ref|	APAF1	True	False	True
	QFFLNLEDPQEDMEVIVK	18	gi|7108333|ref|	APAF1	True	False	True
	QPFPNIVQLGLCEPETSEVYQQAK	24	gi|7108333|ref|	APAF1	True	False	True
	SLLFCDR	7	gi|7108333|ref|	APAF1	True	False	True
	SVLAAEAVR	9	gi|7108333|ref|	APAF1	True	False	True
	SVTDSVMGPK	10	gi|7108333|ref|	APAF1	True	False	True
	TELVGPAHLIHEFVEYR	17	gi|7108333|ref|	APAF1	True	False	True
	TLQVFK	6	gi|7108333|ref|	APAF1	True	False	True
	TVLCEGGVPQRPVVFVTR	18	gi|7108333|ref|	APAF1	True	False	True
	VWNIITGNK	9	gi|7108333|ref|	APAF1	True	False	True
	WEYYLK	6	gi|7108333|ref|	APAF1	True	False	True
	YVVPVESSLGKEK	13	gi|7108333|ref|	APAF1	True	False	True
	YVVPVESSLGK	11	gi|7108333|ref|	APAF1	True	False	True
	YYLHDLQVDFLTEK	14	gi|7108333|ref|	APAF1	True	False	True

Protein	Peptide	Length	Protein Accessio	Gene Symbol	Genespecific	IsoformSpecif	Shared
CIAP	ILTTGENYK	9	gi|4502141|ref|	BIRC2	True	True	False
	LGDSPIQK	8	gi|4502141|ref|	BIRC2	True	True	False
	QAEEMASDDLSLIR	14	gi|4502141|ref|	BIRC2	True	True	False
	TNPYSYAMSTEEAR	14	gi|4502141|ref|	BIRC2	True	True	False
	YDFSCELYR	9	gi|4502141|ref|	BIRC2	True	True	False
	YIPTEDVSGLSLEEQLR	17	gi|4502141|ref|	BIRC2	True	True	False
	STEEAR	6	gi|4502141|ref|	BIRC2;GPI	False	False	True
	AGFYYIGPGDR	11	gi|4502141|ref|	BIRC3;BIRC2	False	False	True
	ELIDTILVK	9	gi|4502141|ref|	BIRC3;BIRC2	False	False	True
	MSTYSTFPAGVPVSER	16	gi|4502141|ref|	BIRC3;BIRC2	False	False	True
	VACFACGGK	9	gi|4502141|ref|	BIRC3;BIRC2	False	False	True
VDAC1	AVPPTYADLGK	11	gi|4507879|ref|	VDAC1	True	True	False
	AVPPTYADLGKSARDVFTK	19	gi|4507879|ref|	VDAC1	True	True	False
	AVPPTYADLGKSAR	14	gi|4507879|ref|	VDAC1	True	True	False
	EHINLGCDMDFDIAGPSIR	19	gi|4507879|ref|	VDAC1	True	True	False
	GALVLGYEGWLAGYQMNFETAK	22	gi|4507879|ref|	VDAC1	True	True	False
	GLKLTFDSSFSPNTGKK	17	gi|4507879|ref|	VDAC1	True	True	False
	GYGFGLIK	8	gi|4507879|ref|	VDAC1	True	True	False
	GYGFGLIKLDLK	12	gi|4507879|ref|	VDAC1	True	True	False
	IKTGYK	6	gi|4507879|ref|	VDAC1	True	True	False
	IKTGYKR	7	gi|4507879|ref|	VDAC1	True	True	False
	KLETAVNLAWTAGNSNTR	18	gi|4507879|ref|	VDAC1	True	True	False
	LETAVNLAWTAGNSNTR	17	gi|4507879|ref|	VDAC1	True	True	False
	LTFDSSFSPNTGK	13	gi|4507879|ref|	VDAC1	True	True	False
	LTFDSSFSPNTGKK	14	gi|4507879|ref|	VDAC1	True	True	False
	LTLSALLDGK	10	gi|4507879|ref|	VDAC1	True	True	False
	LTLSALLDGKNVNAGGHK	18	gi|4507879|ref|	VDAC1	True	True	False
	NVNAGGHK	8	gi|4507879|ref|	VDAC1	True	True	False
	NVNAGGHKLGLGLEFQA	17	gi|4507879|ref|	VDAC1	True	True	False
	REHINLGCDMDFDIAGPSIR	20	gi|4507879|ref|	VDAC1	True	True	False
	SENGLEFTSSGSANTETTK	19	gi|4507879|ref|	VDAC1	True	True	False
	SENGLEFTSSGSANTETTKVTGSLETK	27	gi|4507879|ref|	VDAC1	True	True	False
	SRVTQSNFAVGYK	13	gi|4507879|ref|	VDAC1	True	True	False
	SRVTQSNFAVGYKTDEFQLHTNVNDGTEFGGS	36	gi|4507879|ref|	VDAC1	True	True	False
	TDEFQLHTNVNDGTEFGGSIYQK	23	gi|4507879|ref|	VDAC1	True	True	False
	TDEFQLHTNVNDGTEFGGSIYQKVNK	26	gi|4507879|ref|	VDAC1	True	True	False
	TKSENGLEFTSSGSANTETTK	21	gi|4507879|ref|	VDAC1	True	True	False
	TKSENGLEFTSSGSANTETTKVTGSLETK	29	gi|4507879|ref|	VDAC1	True	True	False
	VNNSSLIGLGYTQTLKPGIK	20	gi|4507879|ref|	VDAC1	True	True	False
	VTGSLETK	8	gi|4507879|ref|	VDAC1	True	True	False
	VTGSLETKYR	10	gi|4507879|ref|	VDAC1	True	True	False
	VTQSNFAVGYK	11	gi|4507879|ref|	VDAC1	True	True	False
	VTQSNFAVGYKTDEFQLHTNVNDGTEFGGSIY(	34	gi|4507879|ref|	VDAC1	True	True	False
	VTQSNFAVGYKTDEFQLHTNVNDGTEFGGSIY(	37	gi|4507879|ref|	VDAC1	True	True	False
	WNTDNTLGTEITVEDQLAR	19	gi|4507879|ref|	VDAC1	True	True	False
	WTEYGLTFTEK	11	gi|4507879|ref|	VDAC1	True	True	False
	WTEYGLTFTEKWNTDNTLGTEITVEDQLAR	30	gi|4507879|ref|	VDAC1	True	True	False
	YQIDPDACFSAK	12	gi|4507879|ref|	VDAC1	True	True	False
	YRWTEYGLTFTEK	13	gi|4507879|ref|	VDAC1	True	True	False
	FGIAAK	6	gi|42476281|ref	VDAC3;VDAC2;VDAC1	False	False	True
Caspase 9	DHGFEVASTSPEDESPGSNPEPDATPFQEGLR	32	gi|14790124|ref	CASP9	True	False	True
	ELFRPHMIEDIQR	13	gi|14790124|ref	CASP9	True	True	False
	GNADLAYILSMEPCGHCLIINNVNFCR	27	gi|14790124|ref	CASP9	True	False	True
	KPEVLRPETPRPVDIGSGGFGDVGALESLR	30	gi|14790124|ref	CASP9	True	False	True
	LFFIQACGGEQK	12	gi|14790124|ref	CASP9	True	False	True
	LSKPTLENLTPVVLRPEIR	19	gi|14790124|ref	CASP9	True	False	True
	QLIIDLETR	9	gi|14790124|ref	CASP9	True	True	False
	VANAVSVK	8	gi|14790124|ref	CASP9	True	False	True
Caspase 8	AQISAYR	7	gi|15718704|ref	CASP8	True	False	True
	CKLDDDMNLLDIFIEMEK	18	gi|15718704|ref	CASP8	True	False	True
	CPSLAGKPK	9	gi|15718704|ref	CASP8	True	False	True
	DALMLFQR	8	gi|15718704|ref	CASP8	True	False	True
	EQDSESQTLDK	11	gi|15718704|ref	CASP8	True	False	True
	FLLQEEISK	9	gi|15718704|ref	CASP8	True	False	True
	FLSLDYIPQR	10	gi|15718704|ref	CASP8	True	False	True
	GDDILTILTEVNYEVSNKDDKK	22	gi|15718704|ref	CASP8	True	False	True
	GDDILTILTEVNYEVSNK	18	gi|15718704|ref	CASP8	True	False	True
	GIIYGTDGQEAPIYELTSQFTGLK	24	gi|15718704|ref	CASP8	True	False	True
	GIPVETDSEEQPYLEMDLSSPQTR	24	gi|15718704|ref	CASP8	True	False	True
	GYCLIINNHNFAK	13	gi|15718704|ref	CASP8	True	False	True
	IINDYEEFSKER	12	gi|15718706|ref	CASP8	True	False	True
	IINDYEEFSK	10	gi|15718704|ref	CASP8	True	False	True
	INRLDLLITYLNTR	14	gi|15718704|ref	CASP8	True	False	True
	KQEPIKDALMLFQR	14	gi|15718704|ref	CASP8	True	False	True
	LDDDMNLLDIFIEMEK	16	gi|15718704|ref	CASP8	True	False	True
	LGDSETAMVPGK	12	gi|122056476|re	CASP8	True	True	False
	MLEESNLSFLK	11	gi|15718704|ref	CASP8	True	False	True
	NLYDIGEQLDSEDLASLK	18	gi|15718704|ref	CASP8	True	False	True
	NPAEGTWYIQSLCQSLR	17	gi|15718704|ref	CASP8	True	False	True
	QEPIKDALMLFQR	13	gi|15718704|ref	CASP8	True	False	True
	QMPQPTFTLR	10	gi|15718704|ref	CASP8	True	False	True
	QTSGILSDHQQSQFCK	16	gi|15718712|ref	CASP8	True	True	False
	VCAQINK	7	gi|15718704|ref	CASP8	True	False	True
	VFFIQACQGDNYQK	14	gi|15718704|ref	CASP8	True	False	True
	VILGEGK	7	gi|15718704|ref	CASP8	True	False	True
	VMLYQISEEVSR	12	gi|15718704|ref	CASP8	True	False	True

Footnote: peptides marked in red were excluded from analysis due to insufficient specificity.

Table S2: Mass spectrometry peptide details (Related to Figure 1).

Protein	Total peptides analyzed	Total gene-specific peptides analyzed	Total gene-specific peptides detected (all tissues)	Total gene-specific peptides detected (Adult B Cells)
BAX	19	18	17	12
BAK	12	12	9	6
BCL-2	7	6	6	5
BCL-XL	8	7	4	0
MCL-1	6	4	4	0
BIM	5	5	4	3
BID	12	12	12	9
APAF-1	54	50	38	16
Caspase 3	23	23	20	7
XIAP	20	20	14	2
CIAP	11	6	3	0
VDAC1	39	38	35	16
Caspase 9	8	8	4	3
Caspase 8	28	28	26	18

A

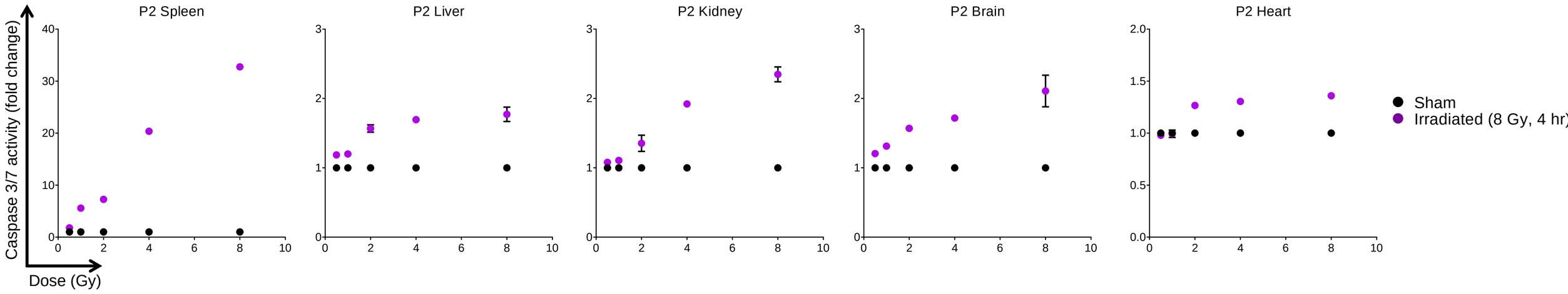
P2 Spleen
P2 Liver
P2 Kidney
P2 Brain
P2 Heart
Caspase 3/7 activity (fold change)
Dose (Gy)
Sham
Irradiated (8 Gy, 4 hr)

B

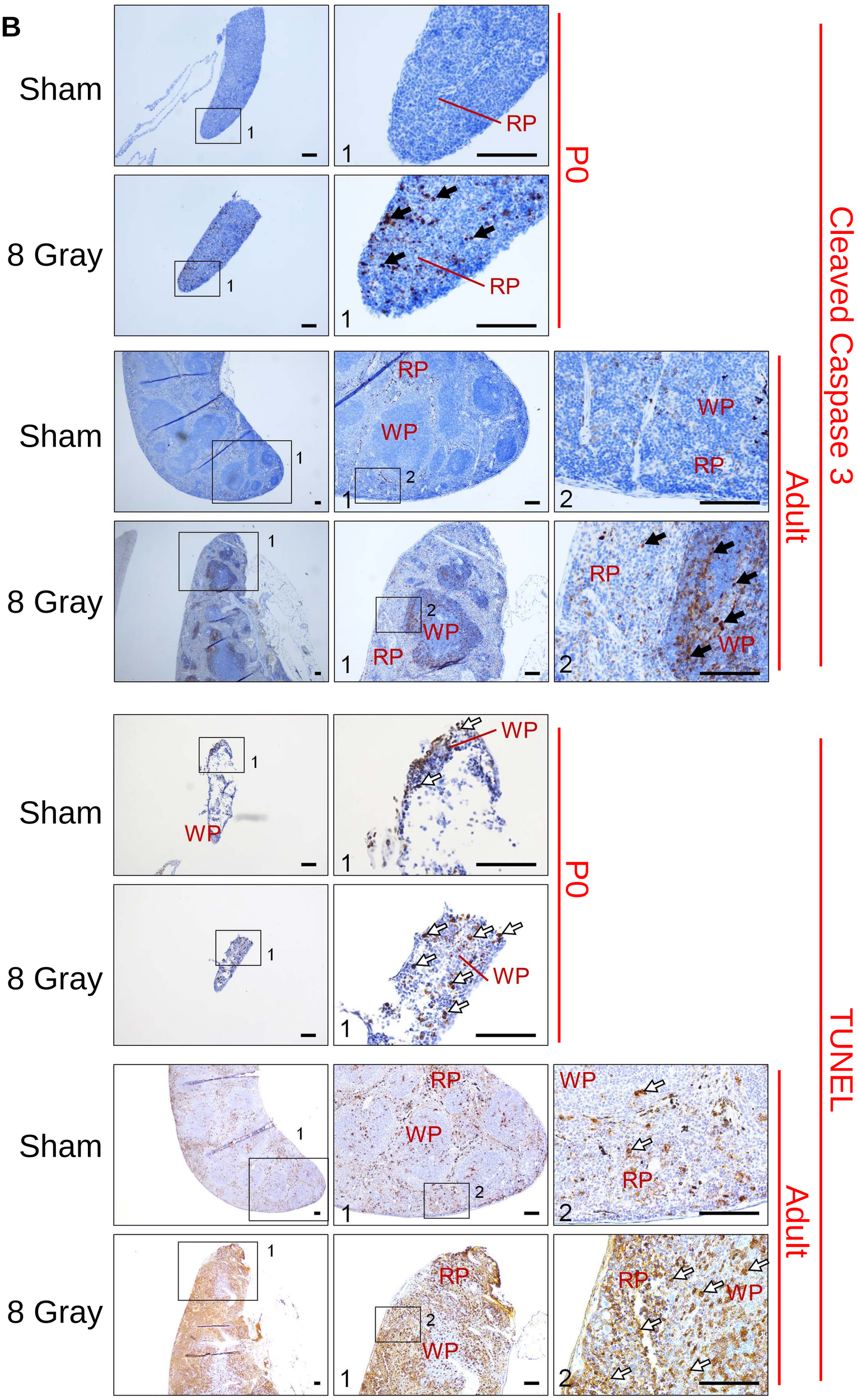
Sham
8 Gray
Sham
8 Gray
Sham
8 Gray
Sham
8 Gray
RP
WP
1
2
P0
Adult
Cleaved Caspase 3
TUNEL

C

Cleaved Caspase 3

P0

Adult

TUNEL

P0

Adult

Sham

8 Gray

Sham

8 Gray

Sham

8 Gray

Sham

8 Gray

HC

HP

TEV

1

2

3

D

Sham

8 Gray

Sham

8 Gray

Sham

8 Gray

Sham

8 Gray

Co
Me
Tu
Glo
1
2

P0

Adult

Cleaved Caspase 3

TUNEL

Cleaved Caspase 3

P0

Adult

E

Sham

8 Gray

Sham

8 Gray

OB

CC

E

Sham

8 Gray

Sham

8 Gray

OB

CC

1

2

3

P0

Adult

TUNEL

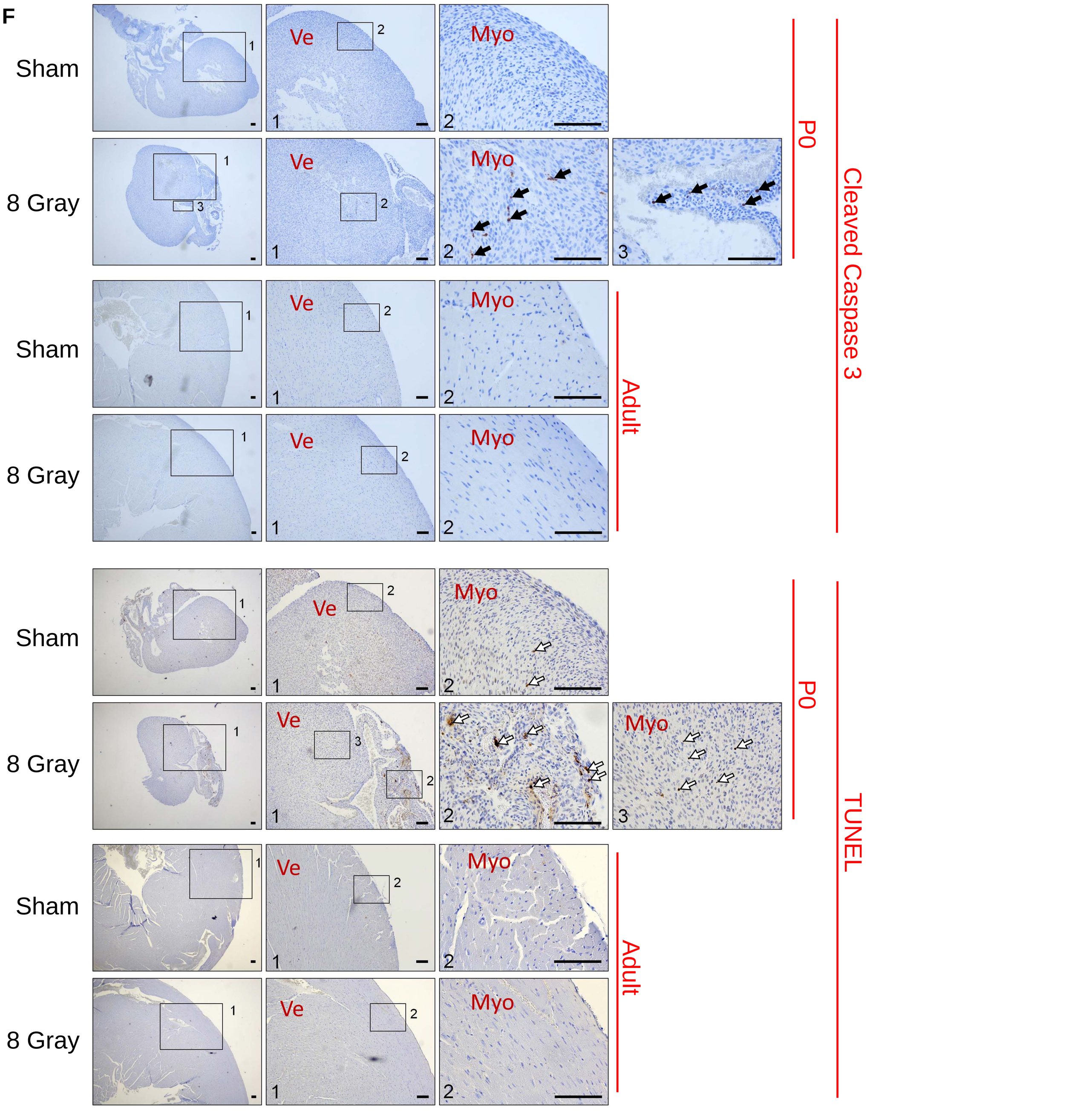

Figure S2: Gamma irradiation induces apoptosis in early postnatal brain, heart, kidney and liver tissue (Related to Figure 2). (A) Mice were irradiated with indicated doses and tissues were collected after four hours and caspase 3/7 activity was measured. Each point represents the mean ± SD of three measurements in each tissue in one experiment. (B-F) After whole body irradiation of neonatal (P0) and adult (P60+) mice, apoptosis was detected in the spleen (B), liver (C), kidney (D), brain (E) and heart (F) by detecting cleaved caspase 3 or TUNEL positivity as indicated. Representative cells undergoing apoptosis are marked with either filled arrowheads (cleaved caspase 3-positive) or white arrowheads (TUNEL^{+}). Scale bars are 200 μm. (B) “RP” designates red pulp while “WP” designates white pulp within spleen. (C) “TEV” designates terminal hepatic venule; “HP” designates hepatocyte plates; “HC” designates hematopoietic cells. (D) “Co” designates kidney cortex; “Me” designates kidney medulla; “Tu” designates tubules; “Glo” designates Glomerulus. (E) “OB” designates olfactory bulb while “CC” designates cerebral cortex. (F) “Ve” designates ventricle while “Myo” designates myocardium. All images are representative of two independent experiments.

A

Sham

8 Gray

RP

WP

RP

P0

BAX

Adult

BAK

B

Sham

8 Gray

Sham

8 Gray

Sham

8 Gray

Sham

8 Gray

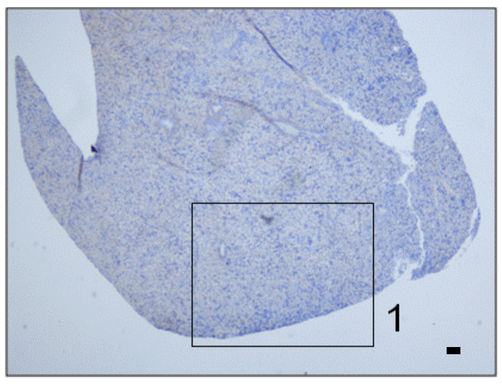

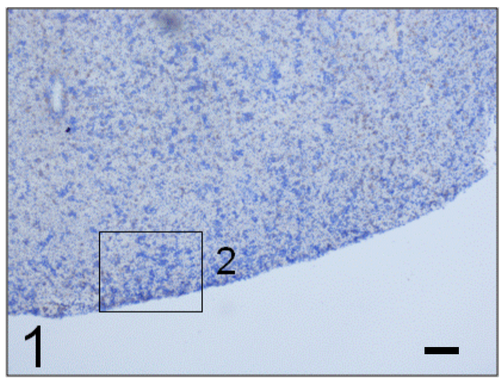

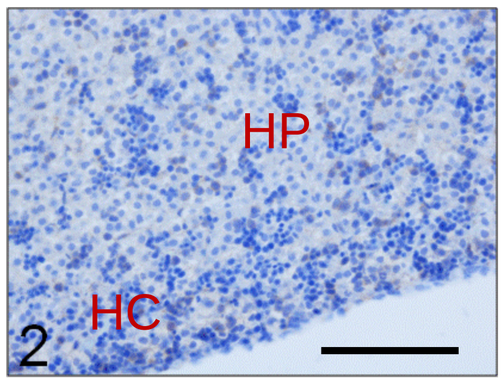

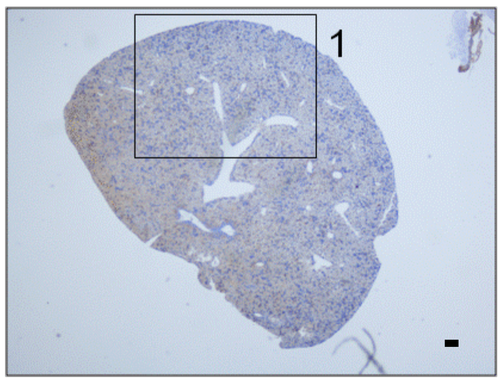

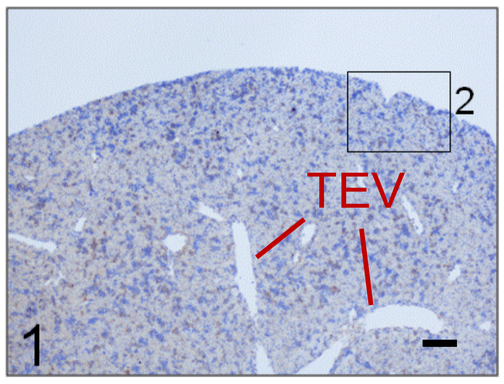

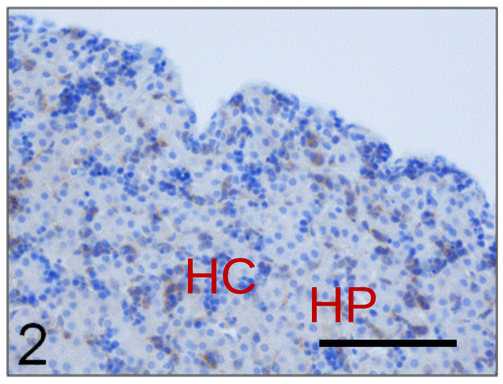

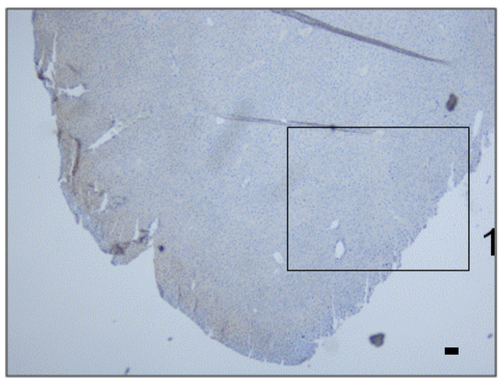

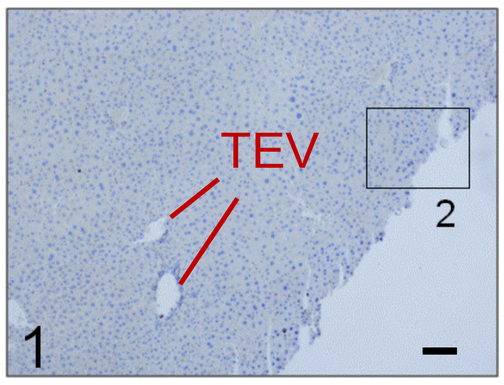

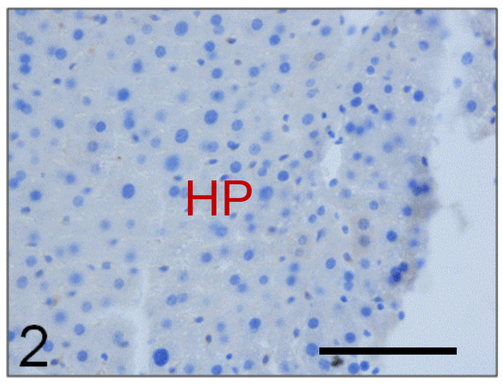

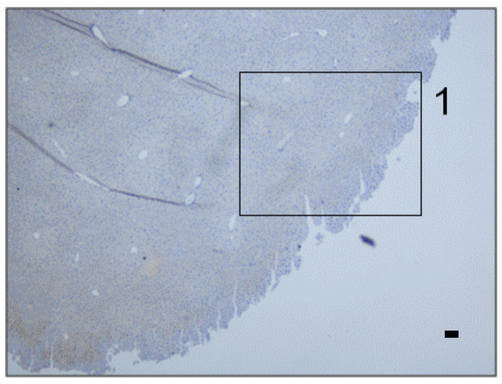

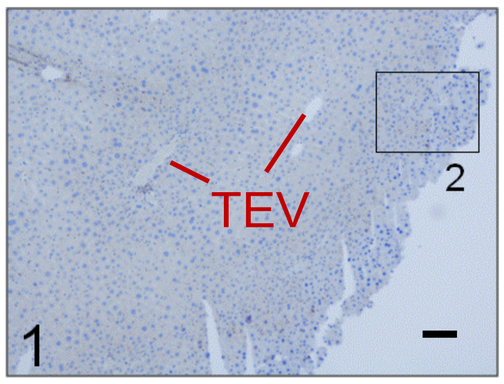

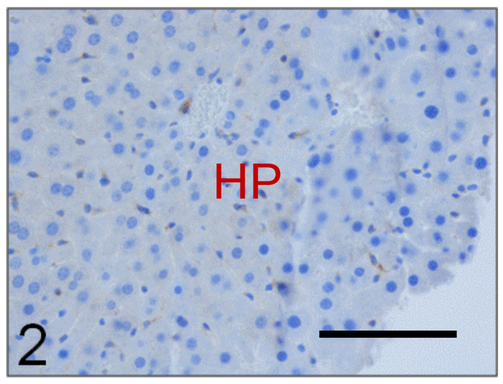

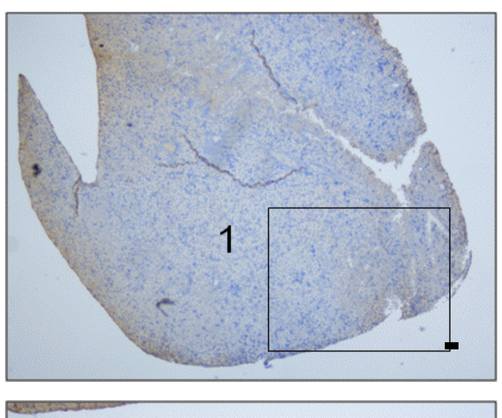

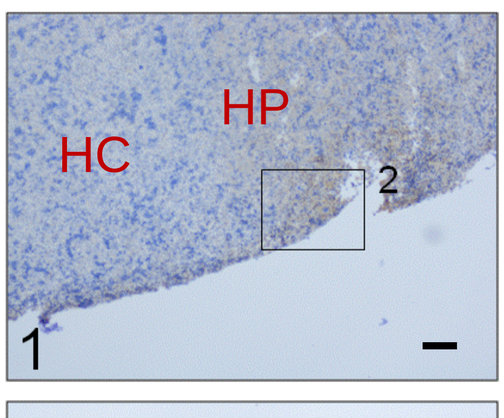

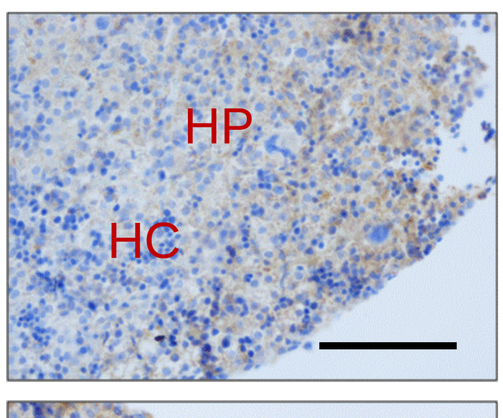

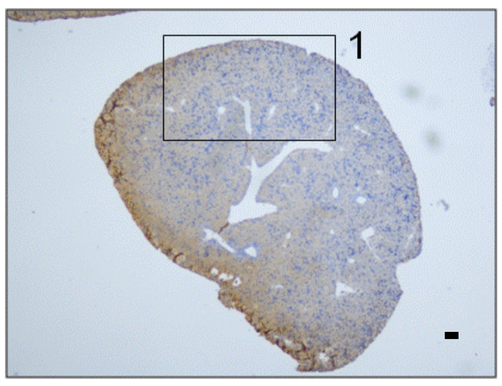

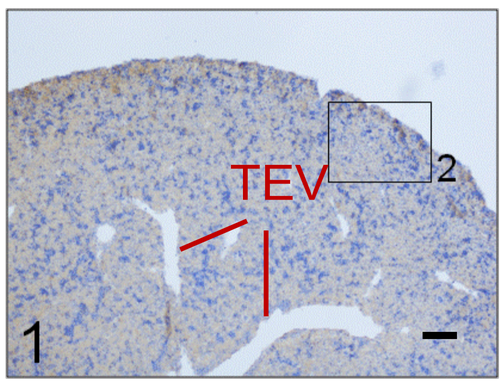

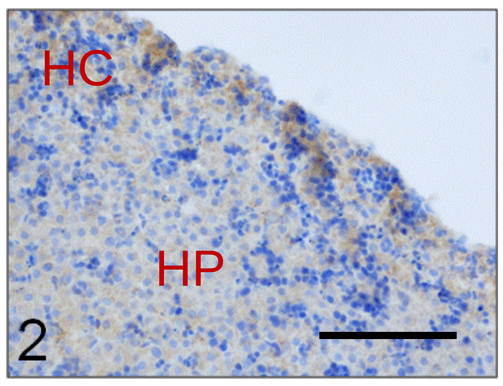

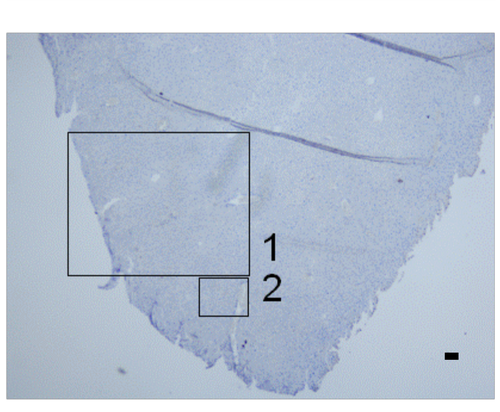

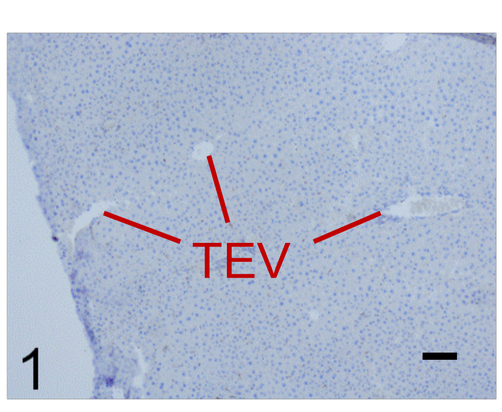

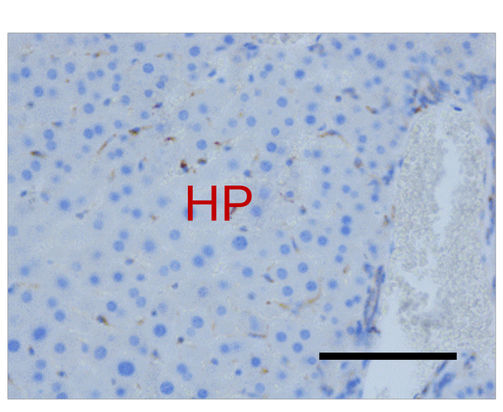

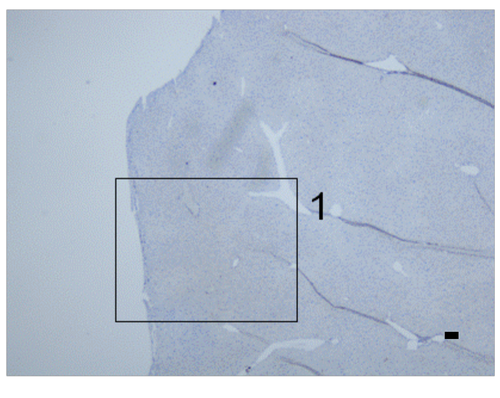

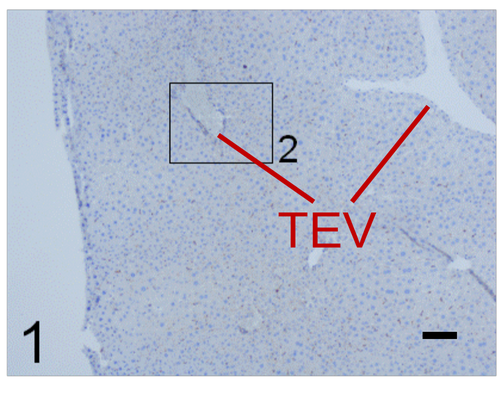

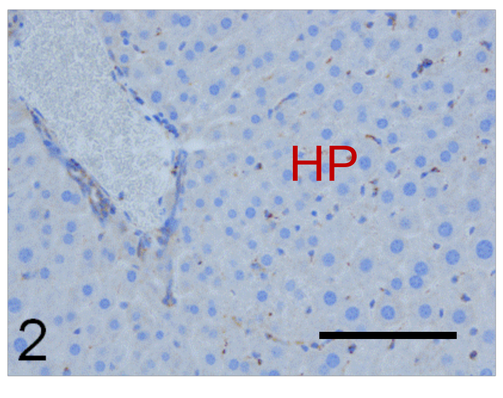

P0

BAX

Adult

P0

BAK

Adult

c

Sham

8 Gray

Sham

8 Gray

Sham

8 Gray

Sham

8 Gray

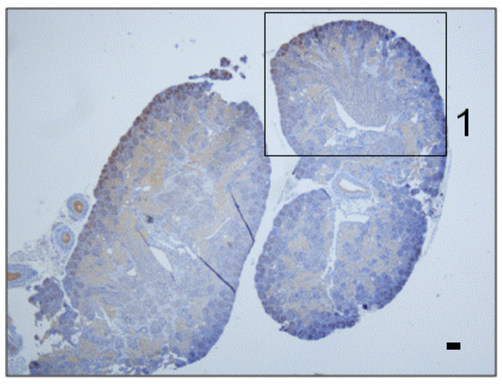

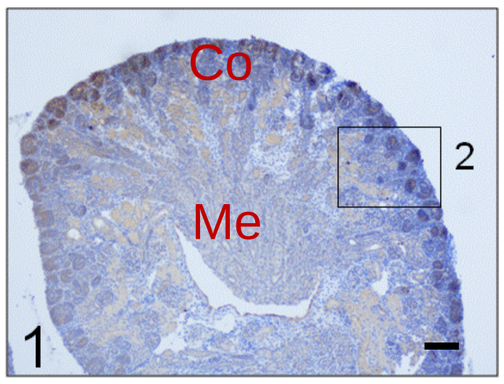

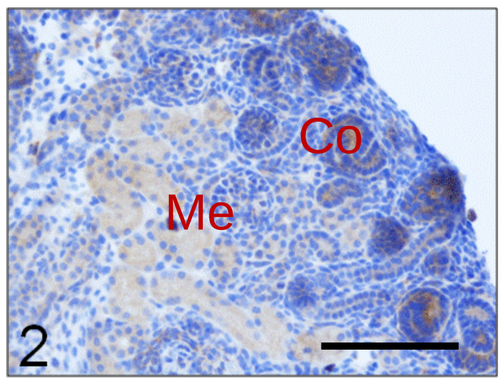

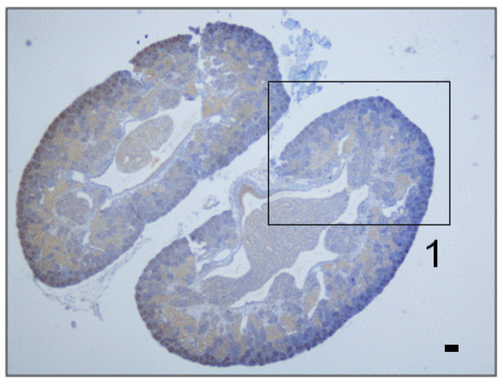

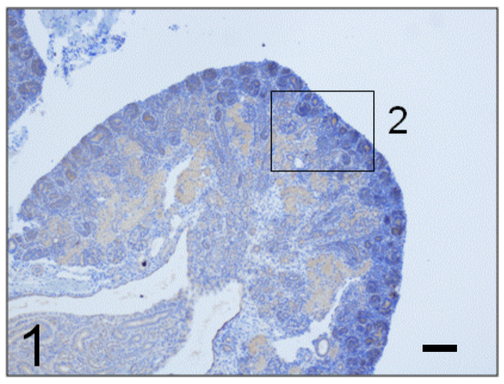

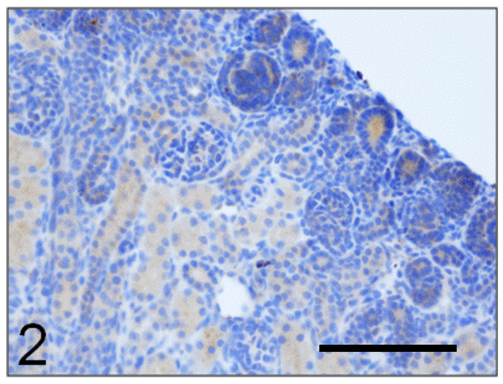

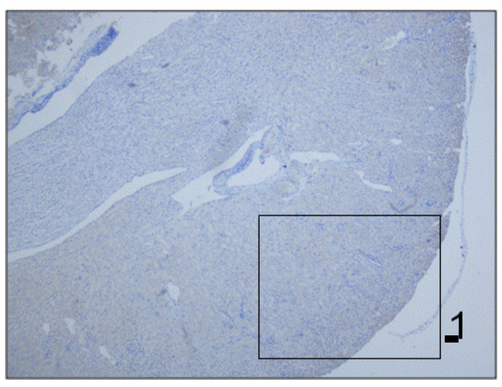

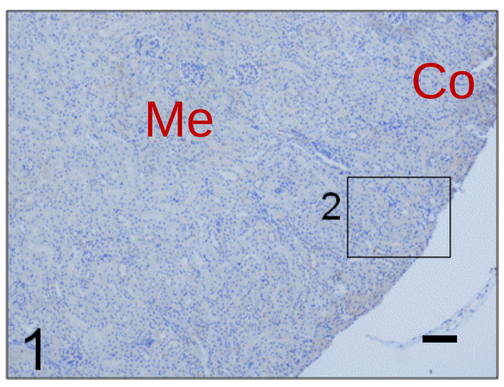

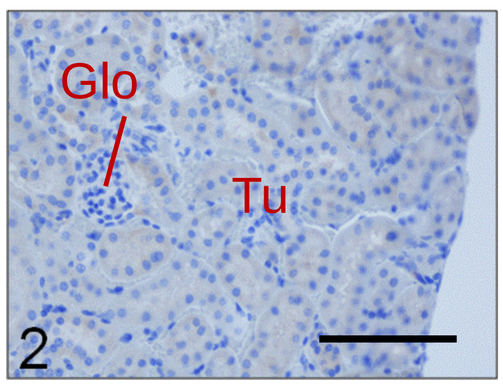

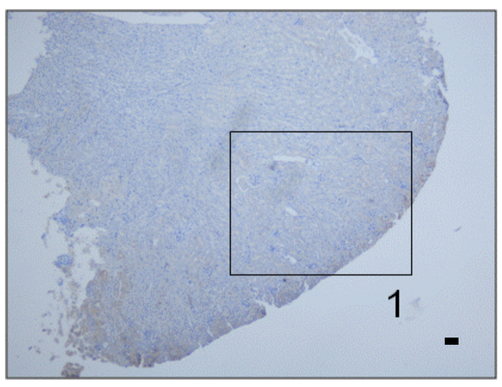

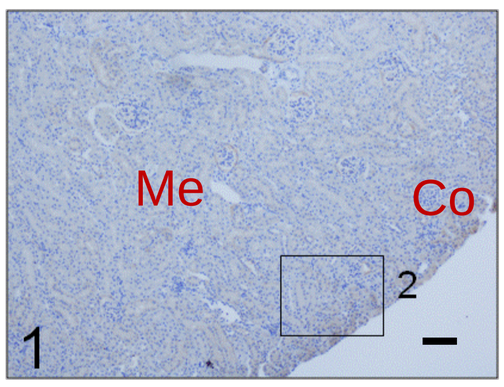

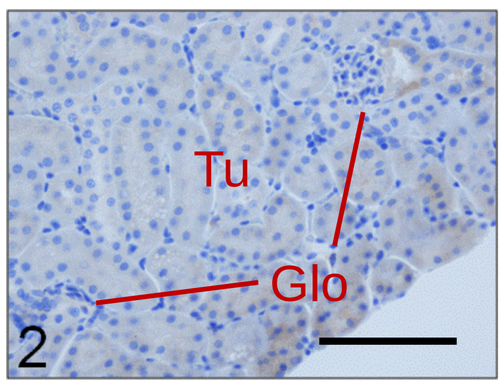

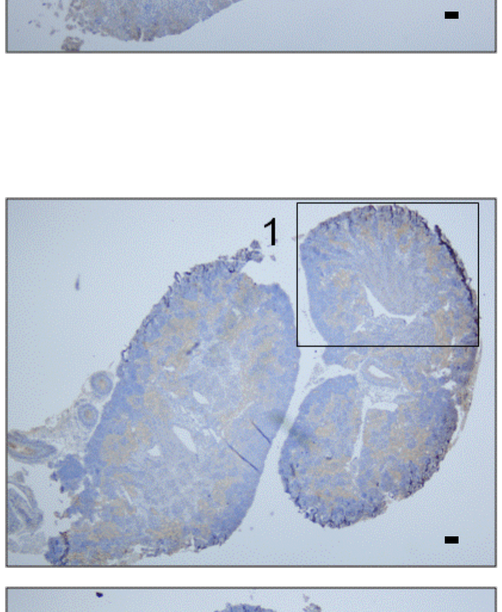

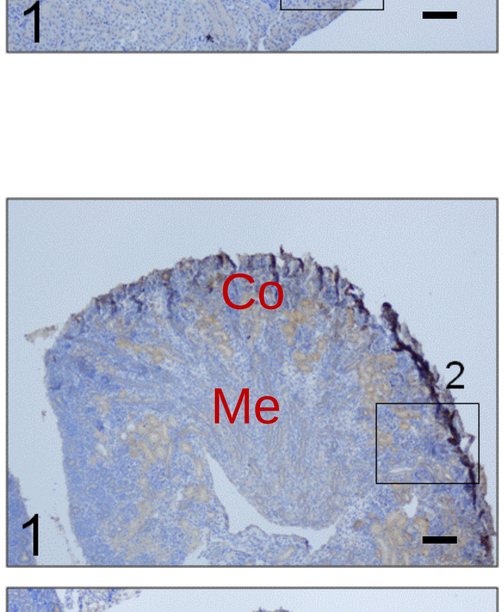

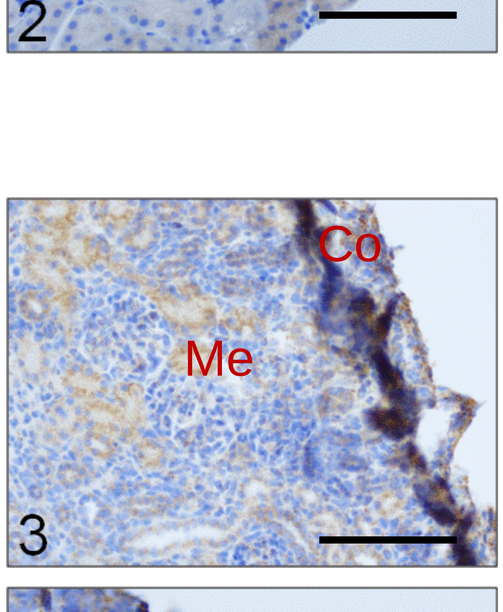

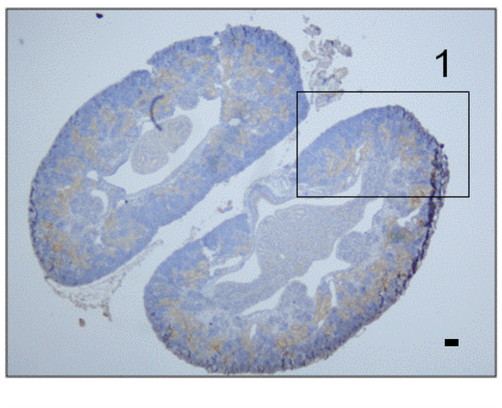

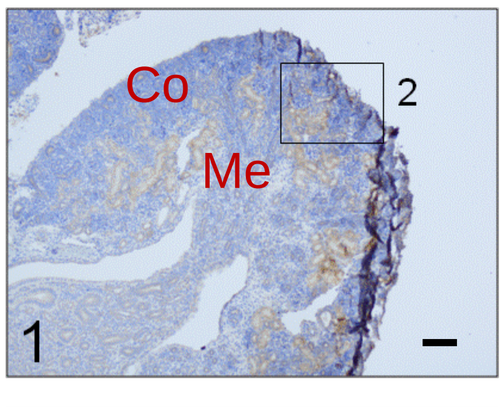

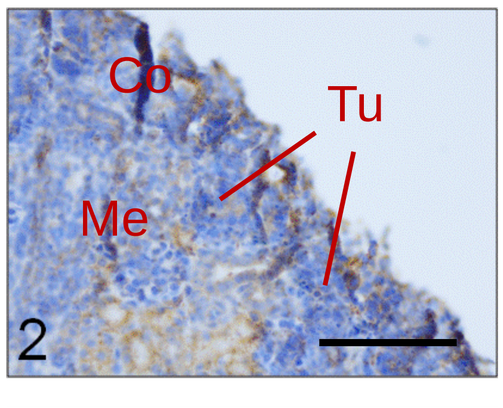

P0

BAX

Adult

P0

BAK

Adult

D

Sham

8 Gray

Sham

8 Gray

Sham

8 Gray

Sham

8 Gray

OB

CC

P0

Adult

BAX

BAK

E

Sham

8 Gray

Sham

8 Gray

Sham

8 Gray

Sham

8 Gray

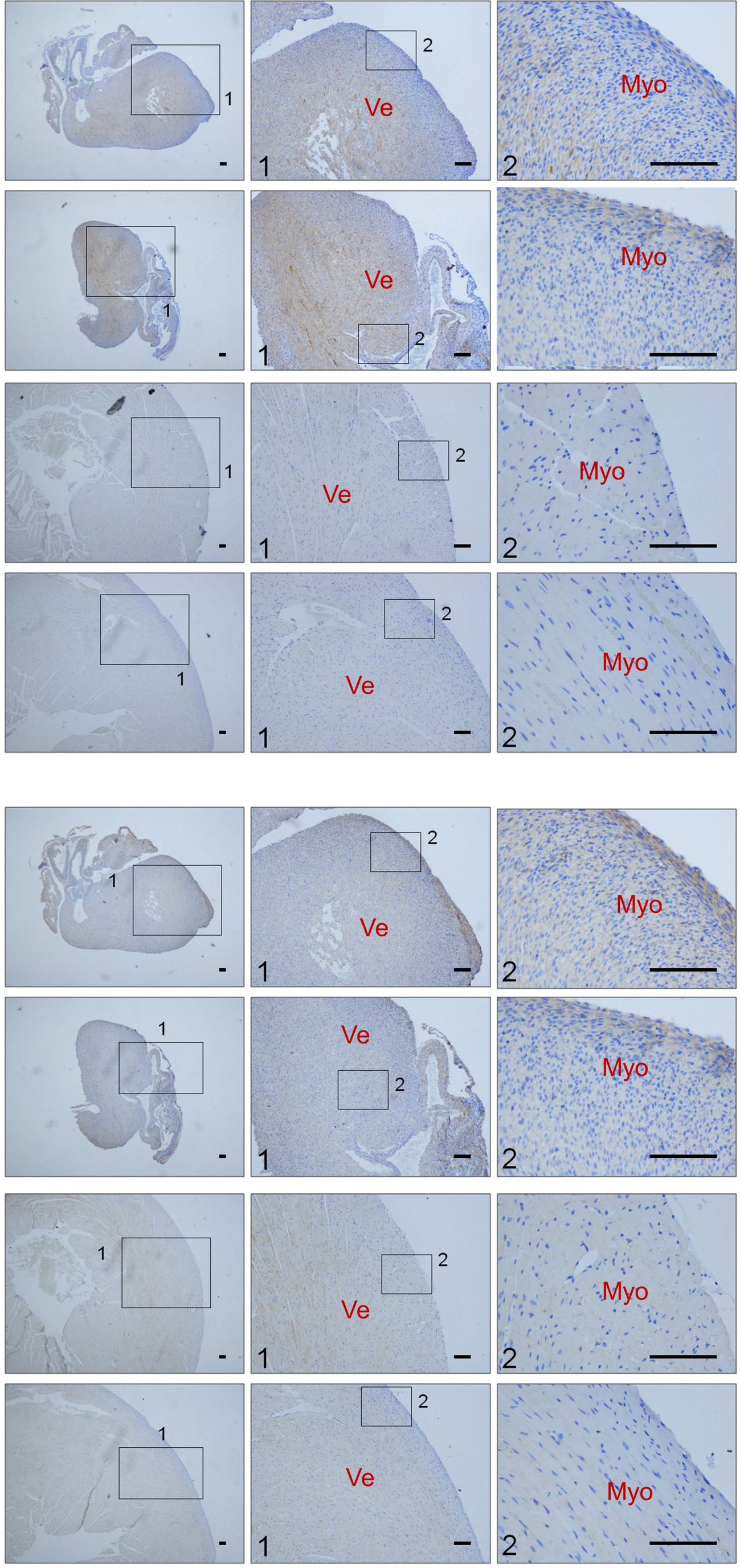

Figure S3: Detection of BAX and BAK in sham treated or irradiated tissue from adult or early postnatal mice (Related to Figure 4). After whole body irradiation, BAX and BAK were stained in the spleen (A), liver (B), kidney (C), brain (D) and heart (E). Brown staining indicates detection of the indicated protein. (A) “RP” designates red pulp while “WP” designates white pulp within spleen. (B) “TEV” designates terminal hepatic venule; “HP” designates hepatocyte plates; “HC” designates hematopoietic cells. (C) “Co” designates kidney cortex; “Me” designates kidney medulla; “Tu” designates tubules; “Glo” designates Glomerulus. (D) “OB” designates olfactory bulb while “CC” designates cerebral cortex. (E) “Ve” designates ventricle while “Myo” designates myocardium. All images are representative of two independent experiments. Scale bars are 200 μm.

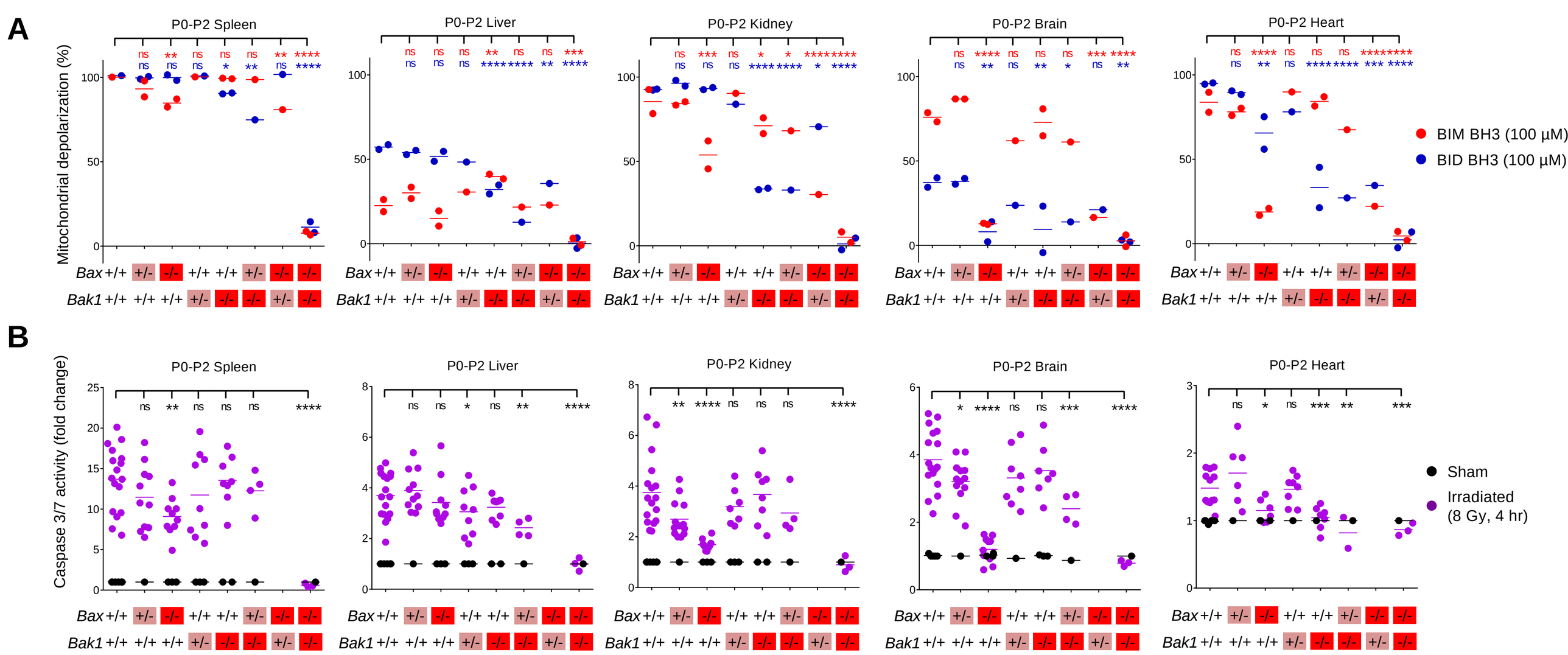

Figure S4: BAX and BAK dependence in early postnatal mouse tissues (Related to Figure 5). (A) Summary BH3 Profiling data from P0-P2 mouse tissues of indicated genotypes. Each point represents the mean of 3 measurements in each tissue across 4 IEs. Horizontal bars represent means. (B) Summary caspase 3 activity data from P0-P2 mouse tissues after whole body irradiation. Each point represents an average of 3 measurements in each tissue across 11 IEs. Horizontal bars represent means.

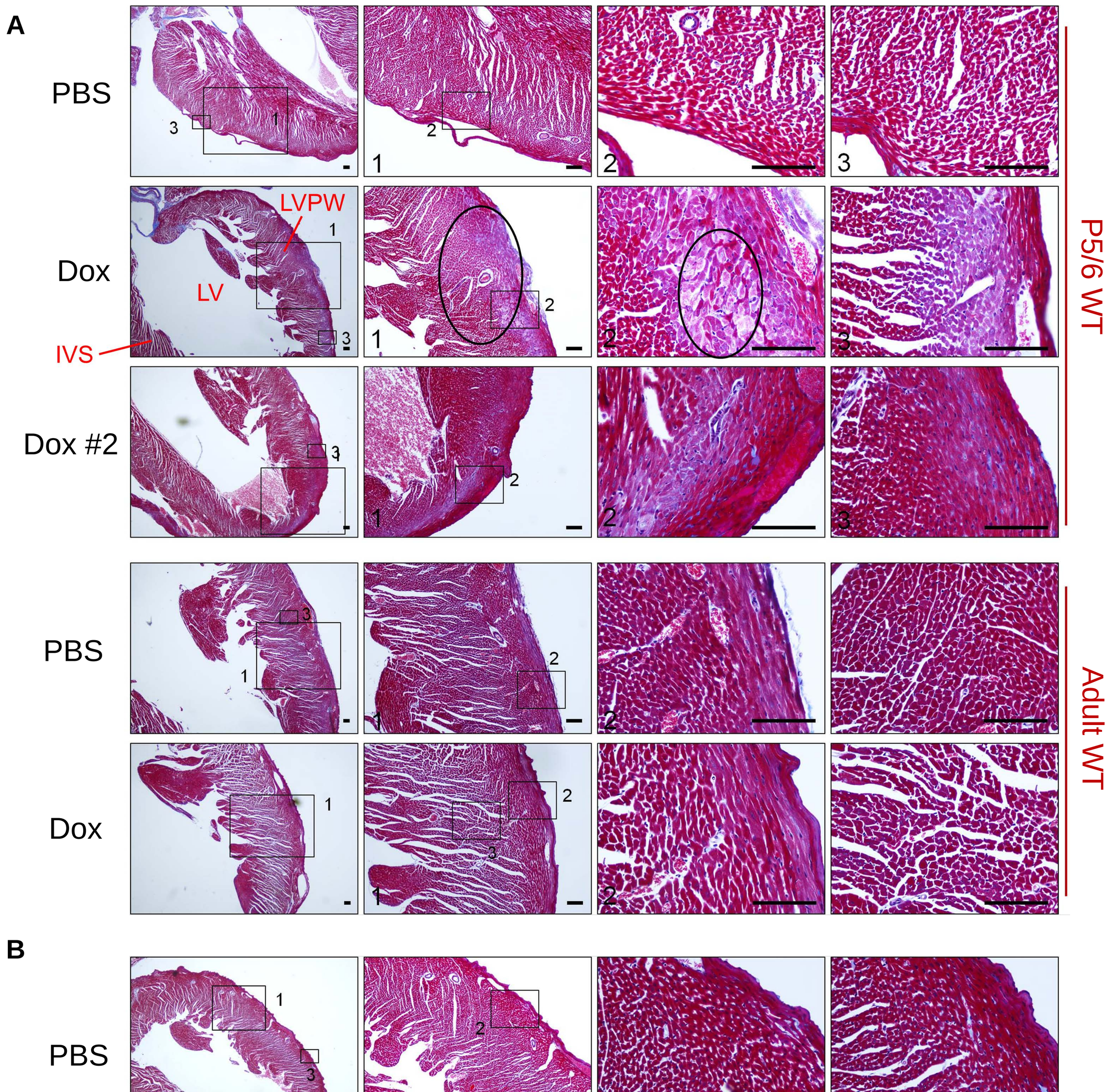

Figure S5: Early postnatal mouse hearts show increased sensitivity to doxorubicin treatment, which is reduced in mice lacking BAX and BAK (Related to Figure 6). (A) Mice of indicated ages were injected with three doses of PBS (vehicle) or doxorubicin (5 mg/kg) and heart tissue was stained with Masson's Trichrome Stain (MTS). (B) P5/6 *Bax*$^{-/-}$ *Bak1*$^{-/-}$ mice were treated as in (A). For general orientation, "LV" designates left ventricle; "IVS" designates interventricular septum; "LVPW" designates left ventricular posterior wall. Black ovals mark the myocardium which shows early signs of injury. These signs of injury include appearance of "foamy cells," altered myocyte structure, myocyte dropout and hypereosinophilic appearance to the myocardium. Note that signs of injury are less apparent in the adult as well as *Bax*$^{-/-}$ *Bak1*$^{-/-}$ mice. Scale bars are 200 μm.

Movie S1: Echocardiogram of WT mouse treated with PBS starting at P5 (Related to Figure 6). Provided as a movie in supplemental materials. A WT mouse was treated with three doses of PBS on day 0, 4, and 7, starting at postnatal day 5 (P5). Echocardiogram was performed at day 14. Movie depicts parasternal long-axis view of beating heart. Normal interventricular septal wall and posterior wall thickness can be observed, along with normal ejection fraction (measurement of how much blood the left ventricle pumps out with each contraction).

Movie S2: Echocardiogram of WT mouse treated with doxorubicin starting at P5 (Related to Figure 6). Provided as a movie in supplemental materials. A WT mouse was treated with three doses of doxorubicin (5mg/kg) on day 0, 4, and 7, starting at postnatal day 5 (P5). Echocardiogram was performed at day 14. Movie depicts parasternal long-axis view of beating heart. Reduced interventricular septal wall and posterior wall thickness can be observed, along with reduced ejection fraction (measurement of how much blood the left ventricle pumps out with each contraction).

Table S3: Human brain specimen details (Related to Figure 7).

Sample ID	Secondary ID (if applicable)	Age	Months post conception	Diagnosis	Laterality	Brain Region	Surgery	BIM BH3 (100µM)	BID BH3 (100µM)
25	N/A	0 years, 4 months	14	Diffuse cortical dysplasia	Right	Temporal lobe	Temporal lobectomy	35.4%	47.5%
4	N/A	0 years, 9 months	19	Sturge-Weber syndrome	Left	Anterior temporal lobe	Functional hemispherectomy	36.2%	32.9%
23	A	0 years, 9 months	19	Perinatal stroke	Left	Medial temporal lobe	Functional hemispherectomy	22.3%	16.6%
23	B	0 years, 9 months	19	Perinatal stroke	Left	Lateral temporal lobe	Functional hemispherectomy	27.5%	13.9%
24	N/A	0 years, 11 months	21	Focal cortical dysplasia	Left	Hippocampus	Anterior temporal lobectomy	26.9%	22.6%
8	N/A	1 year, 0 months	22	Tuberous sclerosis	Left	Temporal lobe	Anterior temporal lobectomy	21.3%	26.7%
3	N/A	1 year, 0.5 months	22.5	Perinatal stroke	Left	Hippocampus	Hemispheric disconnection	24.5%	40.1%
8	N/A	1 year, 7 months	29	Tuberous sclerosis	Left	Lateral temporal lobe	Temporal lobectomy	26.5%	19.3%
14	N/A	1 year, 7 months	29	Focal cortical dysplasia; not otherwise specified	Right	Frontal lobe	Hemispheric disconnection	25.4%	28.4%
18	N/A	1 year, 7 months	29	Focal cortical dysplasia; not otherwise specified	Left	Frontal lobe	Frontal resection	15.6%	16.3%
11	N/A	1 year, 9 months	31	Focal cortical dysplasia IIa	Left	Frontal lobe	Frontal resection	25.9%	26.5%
12	N/A	2 years, 6 months	40	Focal cortical dysplasia; not otherwise specified	Left	Frontal lobe	Functional hemispherectomy with posterior disconnection	20.4%	22.9%
2	N/A	3 years, 10 months	56	Malformation of cortical development	Right	Lateral temporal lobe	Modified perisylvian functional hemispherectomy	22.1%	16.0%
16	B	5 years, 3.5 months	73.5	Focal cortical dysplasia IIa	Left	Intermdiate temporal lobe	Temporal lobectomy	22.6%	19.9%
16	C	5 years, 3.5 months	73.5	Focal cortical dysplasia IIa	Left	Lateral temporal lobe	Temporal lobectomy	17.6%	11.8%
17	A	5 years, 7 months	77	Focal cortical dysplasia Ia	Left	Lateral temporal lobe	Anterior temporal lobectomy	11.5%	6.5%
17	B	5 years, 7 months	77	Focal cortical dysplasia Ia	Left	Hippocampus	Anterior temporal lobectomy	7.7%	8.3%
17	C	5 years, 7 months	77	Focal cortical dysplasia Ia	Left	Parahippocampus	Anterior temporal lobectomy	12.9%	12.2%
7	N/A	5 years, 11 months	81	Rasmussen Encephalitis	Left	Lateral temporal lobe	Functional hemispherectomy	17.2%	21.2%
6	N/A	6 years, 11 months	93	Focal cortical dysplasia IIb	Right	Frontal lobe	Frontal resection	4.7%	19.1%
13	N/A	9 years, 4 months	122	Polymicrogyria	Left	Frontal lobe	Frontotemporal resection	13.8%	10.3%
15	B	14 years, 9 months	187	Stroke - gliosis	Left	Hippocampus	Functional hemispherectomy	2.0%	5.2%
15	C	14 years, 9 months	187	Stroke - gliosis	Left	Parietal lobe	Functional hemispherectomy	6.7%	2.0%
19	A	15 years, 8 months	198	prior tumor - gliosis	Right	Temporal lobe	Anterior temporal lobectomy	8.0%	7.0%
19	B	15 years, 8 months	198	prior tumor - gliosis	Right	Medial temporal lobe	Anterior temporal lobectomy	12.0%	10.0%
1	N/A	18 years, 10 months	236	Focal cortical dysplasia IIb	Left	Frontal lobe	Frontal resection	2.2%	13.8%
9	N/A	19 years, 1 month	239	Gliosis	Left	Temporal lobe	Anterior temporal lobectomy	7.8%	12.9%
10	N/A	21 years, 0 months	262	Trauma - gliosis	Right	Temporal lobe	Anterior temporal lobectomy	0.1%	5.9%
20	N/A	21 years, 0 months	262	Focal cortical dysplasia; not otherwise specified	Left	Temporal lobe	Temporal lobe resection	6.8%	0.3%

Supplemental Experimental Procedures

Mouse strains, breeding and treatments: The following mouse strains were used:
C57BL/6J (WT) (Jackson Laboratories #000664, Bar Harbor ME)
B6.129X1-Baxtm1Sjk/J (*Bax* Knockout) (Jackson Laboratories #002994)
B6.129-Bak1tm1Thsn/J (*Bak1* Knockout) (Jackson Laboratories #004183)
FVB/N-Gt(ROSA)26Sor$^{tm1.1(MYC/ERT2)Gev}$ (Rosa26-MycER^{T2}) (available upon request from Gerard Evan, Cambridge University). Heterozygous male and female mice were bred to produce WT, heterozygous and KO litter-matched animals for analysis. To produce double knockout mice (*Bax*$^{-/-}$, *Bak1*$^{-/-}$) (DKO), male and female *Bax*$^{+/-}$, *Bak1*$^{-/-}$ mice were bred (DKO males and females as well as *Bax*$^{-/-}$ males are sterile). DKO mice were born at Mendelian frequencies, as previously reported (Lindsten et al., 2000), but experienced frequent perinatal lethality, with only a subset surviving to adulthood. Genotypes were confirmed with PCR of DNA samples from tail snips (Transnetyx, Cordova TN). For irradiation experiments, litter-matched mice were placed in an acrylic irradiation pie cage (Braintree Scientific, Braintree MA) and irradiated in a Gammacell 40 “Extractor” (Best Theratronics Ltd., Ottawa, ON Canada) for the time required to deliver the desired dose. Acute doxorubicin (Sigma-Aldrich) treatments (to assess levels of apoptosis soon after dosing) were done by injecting litter-matched mice intraperitoneally (IP) with one dose of the agent at 25 mg/kg or an equal volume of saline. Animals were sacrificed 24 hr later and tissues were collected for downstream analysis (see below). Long-term doxorubicin treatments (to assess heart function via echocardiogram) were done by injecting litter-matched P5/6, P11/12 or adult (P60-P90) mice intraperitoneally with 3 doses of the agent at 5 mg/kg or an equal volume of saline on days 0, 4, and 7, followed by echocardiograms (see below) on day 14. For acute activation of MycER^{T2}, tamoxifen dissolved in peanut oil was injected daily at 40 mg/kg.

Human brain specimens: Patients underwent surgery for removal of seizure foci at Boston Children’s Hospital (Table S3) and resected tissues were first delivered to a neuropathologist for evaluation. If available, a de-identified sample (0.2-0.5 g) of brain tissue was provided to study investigators in PBS on ice and was immediately processed for BH3 Profiling. Part of the sample (0.1 g) was excluded for cryopreservation and was subsequently prepared for immunoblotting. The remaining brain tissue was dissociated by repeated pipetting until a single cell suspension was achieved and BH3 Profiled as outlined above.

Tissue isolation from mouse: All mice were euthanized by CO_2 asphyxiation (mice that were less than 14 days old were decapitated following CO_2 administration). To isolate relevant cells from spleen and thymus, organs were mechanically separated in cold PBS using a Potter-ELV tissue grinder (Wheaton, Millville NJ). For bone marrow, femurs were removed and cold PBS was pipetted into one end and allowed to flow through into a collection receptacle and subjected to red blood cell (RBC) lysis using RBC lysis reagent (Qiagen, Germantown MD) according to manufacturer’s instructions. For peripheral blood mononuclear cells (PBMCs), blood was collected from the mouse immediately post mortem, pipetted into cold PBS and subjected to RBC lysis. For heart, kidney, liver, small intestine, large intestine, and lungs, the organ was first coarsely separated and placed into 50 mL of cold PBS, vortexed and then strained through a 70 µM filter to remove leukocytes

and cell debris (flow through). Tissue remaining in the strainer was then mechanically separated using a Potter-ELV tissue grinder. For brain, tissue was placed into cold PBS and repeatedly pipetted (~20 times) until completely dissociated. Aliquots of single cell suspensions were immobilized on a glass slide using cytospin protocol (ThermoFisher Scientific, Waltham MA) stained with Jorvet Dip Quick Stain (Jorgensen Laboratories, Loveland CO), and examined by a trained pathologist (D.R.C.) for >95% purity (less than 5% of cells of hematopoietic origin). In many tissues, all cells analyzed were of the same type, such as hepatocytes in the liver and cardiomyocytes in the heart. Processing time and protocols per tissue type did not differ between neonatal and adult tissues, and total number of tissues processed in batches was limited to ensure processing time was kept below a maximum of 2 hr from time of tissue collection to start of downstream applications including BH3 Profiling or lysate preparation.

Fluorescence-based BH3 Profiling: 15 µL of BH3 peptides or recombinant proteins (see below for peptide sequences) in T-EB (300 mM Trehalose [Sigma-Aldrich, St. Louis MO], 10 mM Hepes-KOH pH 7.7 [Sigma-Aldrich], 80 mM KCl [Sigma-Aldrich], 1 mM EGTA [Sigma-Aldrich], 1 mM EDTA [Sigma-Aldrich], 0.1% BSA [Sigma-Aldrich], and 5 mM succinate[Sigma-Aldrich]) was deposited into each well in a non-treated, black 384-well plate, 1 treatment per well, in triplicate for each independent experiment. Single cell suspensions were washed once with T-EB before being resuspended at 4X their final density of 6.75 x 10^5 cells/mL. One volume of the 4X cell suspension was added to one volume of a 4X dye solution containing 4 µM JC-1 (Enzo Life Sciences, Farmingdale NY), 40 µg/ml oligomycin (Sigma-Aldrich), 0.02% digitonin (Sigma-Aldrich), and 20 mM 2-mercaptoethanol (Life Technologies) in T-EB. The resulting 2X cell/dye solution was kept at room temperature for 5 min to allow for cell permeabilization and dye equilibration. 15 µL of the 2X cell/dye mix was then added to each treatment well of the 384-well plate, shaken for 15 seconds inside the plate reader, and the fluorescence at 590 nm was measured every 5 min at 32°C. Peptide treatments that were used corresponded to the BH3 domains of the BCL-2 family proteins, and their respective sequences are as follows: BIM: MRPEIWIAQELRRIGDEFNA; BID: EDIIRNIARHLAQVGDSMDR (New England Peptide, Gardner MA). Relative mitochondrial depolarization was defined as the magnitude of mitochondrial depolarization resulting from BH3 peptide treatment as compared to vehicle DMSO (Sigma-Aldrich) and positive control FCCP (p-trifluoromethoxy carbonyl cyanide phenyl hydrazone) (Sigma-Aldrich). The percentage of mitochondrial depolarization was calculated by comparing the JC1 signal (mitochondrial polarization) in cells treated with each peptide or protein concentration in the following manner:

% Mitochondrial Depolarization = [R(t) - F(t)] / [R(t) – FCCP(t)] * 100

where R(t) is the fluorescence value in the reference sample (DMSO), F(t) is the fluorescence value in the test sample (peptide or protein) and FCCP(t) is the fluorescence value in the positive control sample (FCCP) at a time (t) and averaged during the course of the BH3 Profiling assay (from t=20 to 120 min).

Immunoblotting: Immunoblotting was performed as previously described (Montero et al., 2015) Briefly, protein lysates were obtained by cell lysis in Radio Immuno Precipitation Assay (RIPA) buffer (150 mM sodium chloride, 1.0% NP-40, 0.5% sodium deoxycholate,

0.1% sodium dodecyl sulphate, 50 mM Tris, ph 8.0). Protein loading was measured by Protein Assay Dye Reagent (Bio-Rad). Protein samples were electrophoretically separated on NuPAGE 4-12% Bis-Tris polyacrylamide gels (Invitrogen). Heatmaps were generated by normalizing band intensity to loading control (GAPDH). Antibodies used include: BAX (Cell Signaling Technology #2772, Danvers MA); BAK NT (Millipore, Billerica MA); BIM (Cell Signaling Technology #C34C5); BID (clone 11958), BCL-2 3F11 (BD Biosciences, San Jose CA), BCL-X_L (Cell Signaling Technology #2764), MCL-1 (Rockland Immunochemicals, 600-401-394S), APAF-1 (BD Biosciences), Caspase 3 (Cell Signaling Technology #8G10), Caspase 8 (Cell Signaling Technology #4790),Caspase 9 (Cell Signaling Technology #9508), VDAC (Cell Signaling Technology #4661), XIAP (BD Biosciences #610763), CIAP1 (Cell Signaling Technology #4952), c-Myc (Cell Signaling Technology #13987, Santa Cruz Biotechnology #sc-764, Dallas TX), GAPDH (Cell Signaling Technology #5174).

Echocardiograms: Echocardiograms were obtained at 14 days following initiation of sham or doxorubicin treatment with a Vevo 2100 Imaging digital ultrasound system (VisualSonics, Toronto ON Canada) using a 22-55 MHz (MS550D) for adult and 30-70 MHz (MS700) transducer for neonatal mice, as previously described (Bauer et al., 2011). Prior to echocardiography, each mouse chest wall was shaved. Adult and neonatal mice were then placed on a heated platform in the supine position. Echocardiographic analysis was performed on mice receiving oxygen at a heart rate between 400 and 700 beats/min. Data acquisition was initiated with the parasternal cardiac long axis view followed by transition to a short axis view, at the level of mid-papillary muscles. Echocardiographic measurements were obtained from short axis B-mode images. All data were acquired and analyzed in a blinded fashion.

In vitro chemosensitivity assays: For drug-induced, in vitro chemosensitivity assays, neurons were plated in 48-well plates and treated with indicated concentrations of Doxorubicin or Staurosporine (Sigma-Aldrich) for 24 hr. Caspase 3/7 Glo Assay (Promega, Madison WI) was then performed according to manufacturer's instructions and luminescence was measured on a Safire2 microplate reader (Tecan, Männedorf Switzerland). Luminescence readings were normalized to untreated control cells.

Human protein expression data: Fourier-transform mass spectrometry protein expression data in adult and fetal human tissues generated by Kim, et al. (Kim et al., 2014), was downloaded via the humanproteomemap.org website on November 11th, 2014 and again on June 1st, 2015 for local analysis. Expression of relevant proteins in adult and fetal tissues was assessed by examining peptide-level data for each protein, with data excluded from any peptides that were not gene-specific (Table S1 and S2). Spectral counts for all gene-specific peptides were summed and heatmaps were generated by normalizing to the summed spectral count of the tissue displaying the highest expression of each protein analyzed.

Gene expression data in human brain: RNA sequencing (RNA-Seq) data generated across 13 developmental stages in 8-16 brain structures by Miller, et al. (Miller et al., 2014) was downloaded via the brainspan.org website on December 17, 2013 for local analysis. mRNA expression of *BAX* was examined across all brain regions and from the earliest available data (8 weeks post conception) to adulthood (23 years of age). All samples were from

pathologically normal donors. Additional details and documentation is available at brainspan.org.

Statistical analysis: two-way ANOVA (including Fisher's Least Significant Difference [LSD] test for multiple comparisons) was performed using the GraphPad Prism software (GraphPad Software, La Jolla CA). Significance: * $p < 0.05$; ** $p < 0.01$; *** $p < 0.001$; **** $p < 0.0001$.

Rat primary hippocampal neuronal cultures: Neurons were prepared and grown as described previously (Minogue et al., 2009; Walsh et al., 2009). Hippocampi were explanted from E18 Sprague Dawley rat pups in Hank's balanced salt solution and dissociated using 0.25% trypsin (Invitrogen, Carlsbad, CA) for 16 min at 37°C. Neurons were plated at a density of 3x104 cells on the inner 24 wells of poly-D-lysine coated 48-well plates and cultivated in Neurobasal medium supplemented with 0.5 mM Glutamax-I (Invitrogen, Carlsbad, CA) and B27 with antioxidants (Invitrogen, Carlsbad, CA). Five days after plating, 20 µM of 5-fluoro-2'-deoxyuridine was added to reduce glial proliferation. Cultures were kept in a humidified incubator at 37°C and 5% CO2 and once per week half of the media was replaced with fresh Neurobasal medium containing 0.5 mM Glutamax-I and B27 with antioxidants (Kaech and Banker, 2006). Every 3 days after plating, cells from a single well were collected using 0.25% trypsin, washed once with phosphate-buffered saline, and BH3 Profiled as outlined above.

Production and purification of cBID, BIML, and BAX: cBID was produced as previously described (Zha, 2000) with these modifications: 1) BID was cloned into pet16b; 2) cBID was eluted from the column with imidazole. For BIML, the cDNA encoding full-length wildtype murine BIML was cloned into pBluescript II KS(+) vector (Stratagene, Santa Clara CA). DNA sequences encoding a polyhistidine tag followed by a TEV protease recognition site (MHHHHHHGGSGGTGGSENLYFQGT) and an intein/chitin-binding domain were added to the plasmid such that the new plasmid encoded a fusion protein with both an N-terminal His tag and Tev site and an intein/chitin-binding domain at the C-terminus of BIML. The recombinant construct was expressed in SoluBL21 Escherichia coli strain (Genlantis, San Diego CA). Lysis of E. coli was achieved by mechanical disruption with a French press. After affinity chromatography with a chitin column, intein self-cleavage and release of BIML from its fusion partner intein-CBD was initiated by incubation with buffer containing 100 mM β-mercaptoethanol for 36 hr. This process leaves no additional amino acid residues on the C-terminus of BIML. The elution fraction from chitin column was then applied to a Nickel-NTA column (Qiagen, Valencia CA) and BIML was eluted from the Ni column with buffer containing 20 mM HEPES (pH 7.4), 100 mM NaCl, 20% glycerol, 0.3% CHAPS, and 300 mM imidazole. The purified BIML protein was dialyzed against 20 mM HEPES (pH 7.4), 100mM NaCl and 20% glycerol, then flash-frozen and stored at -80 °C. Recombinant BAX was produced as previously described (Suzuki et al., 2000).

Immunohistochemistry: Tissues were collected from mice and immediately placed into 8% formaldehyde solution (Electron Microscopy Sciences, Hatfield PA) and incubated on a rotator for 24 hr at 4°C. The formaldehyde was then replaced with cold PBS and incubated for another 24 hr at 4°C and then stored at 4°C until analysis. Tissues were paraffin embedded and cut into 4µM-thick sections. Slides were stained on the Leica Bond III

autostaining platform using the Bond Polymer Refine Detection kit (Leica, Chicago, IL). Antigen retrieval was performed online using Bond Epitope Retrieval 1 (Leica, Chicago, IL) for 30 min. Slides were then incubated at room temperature with primary antibodies against Cleaved Caspase 3 (Cell Signaling Technology #9664), BAX (Cell Signaling Technology #2772) for 60 min, or BAK (Cell Signaling Technology #12105) for 30 min diluted in Bond Primary Antibody Diluent (Leica, Chicago, IL). Primary antibodies were detected with Post Primary, followed by Polymer-HRP reagents from the Polymer Refine Detection Kit. Slides were developed in Diaminobenzene for 10 min.

TUNEL: Formalin-fixed paraffin tissue sections were stained for terminal deoxynucleotidyl transferase-mediated dUTP nick end labeling (TUNEL) with the ApopTag Peroxidase In Situ Apoptosis Detection Kit (R&D Systems, Minneapolis MN) according to the manufacturer's instructions. At least five views in each slide were randomly selected and quantified for positive staining. Two animals in each group were studied. Results were presented as TUNEL-positive cells per 40X field of view.

Heart histology: Harvested hearts were arrested in diastole with 3 M KCl and fixed with 8% buffered formaldehyde solution and incubated on a rotator for 24 hr at 4°C. The formaldehyde was then replaced with cold PBS and incubated for another 24 hr at 4°C and then stored at 4°C until analysis. Hearts were then embedded in paraffin for analysis by histology. Samples were sectioned at the Histology Core Facility at Beth Israel Deaconess Medical Center. Masson's trichrome staining (MTS) was performed according to the manufacturer's protocol (Sigma-Aldrich, St Louis MO).

Flow-cytometry based BH3 Profiling with intracellular c-Myc staining: Tissues were collected and added to 500 µL PBS on ice. To remove blood, samples were crudely separated, and vortexed in fresh, cold PBS solution three times. Samples were then removed from solution and mechanically separated until finely dissociated, at which time PBS was added to the sample and pipetted repeatedly for further dissociation. The samples, in solution, were then run through a 45 µm filter to ensure single cell suspension. Samples were centrifuged for 5 min at 500xg, resuspended in FACS staining buffer (PBS, 2 mM EGTA, 2% FBS), and stained on ice for 15 min with AF594 anti-mouse CD45 antibody at 1:100 dilution (Biolegend #103144). Samples were then centrifuged for 5 min at 500xg and resuspended in Newmeyer buffer (300 mM Trehalose, 10 mM HEPES-KOH, 80 mM KCl, 1mM EGTA, 1 mM EDTA, 0.1% BSA, 5 mM Succinate, ph 7.7). Flow cytometry-based BH3 Profiling was then performed as previously described (Ryan and Letai, 2013). Samples were added to a 96 well, V-bottom plate (Corning #3897) containing titrated doses of the BIM and/or BID BH3 peptide and positive and negative controls, all in 0.02% digitonin. The plate was then incubated at 28°C for 1 hr. Peptide exposure was terminated by adding 8% formaldehyde in PBS at 1:4 ratio (2% final concentration of formaldehyde). After 15 min, formaldehyde was neutralized with N2 buffer (1.7 M Tris base, 1.25 M Glycine, ph 9.1). 4x Intracellular Staining buffer with TritonX-100 (PBS, 1% Saponin, 10% BSA, 20% FBS, 0.02% Sodium Azide, 2% TritonX-100) was added to each well. The following antibodies were added to all wells except for unstained control wells at the dilutions indicated: Cytochrome c at 1:1000 (ThermoFisher, clone 6H2.B4 with AF647 tag), Hoechst 33342 at 1:2000 (Life technologies #H3570), c-Myc at 1:1000 (Cell Signaling Technology #13987 [rabbit mAb]). Plate was sealed with an adhesive cover and left to stain

overnight at 4°C. Plate was then centrifuged at 500xg for 5 min and the wells were aspirated, leaving behind the cell pellet. Cell pellet was washed once in FACS staining buffer, centrifuged again, and resuspended in 4x Intracellular Staining buffer with TritonX-100 containing anti-rabbit IgG secondary antibody with AF488 tag at 1:1000 (Life technologies #A11070). Plate was sealed with an adhesive cover and left to stain overnight at 4°C. Plate was then centrifuged at 500xg for 5 min and washed with FACS staining buffer twice, then cells were resuspended in FACS staining buffer for analysis on a BD Biosciences LSR II flow cytometer (BD Biosciences).

ChIP-qPCR: Analysis of Myc occupancy on enhancer boxes of promoters of genes of interest was carried out using Active Motif's ChIP-IT qPCR Analysis Kit (Active Motif, Carlsbad, CA) according to manufacturer's instructions using 30 ug of mouse tissue chromatin from each organ (P0 spleen, liver, heart, kidney and brain; adult spleen, kidney and brain) and 25 ul of anti-c-Myc antibody (Santa Cruz Biotechnology sc-764). qPCR was performed using one positive control primer pair (Mybbp1a) and a negative control primer pair that amplifies a region in a gene desert on chromosome 6 (Untr6), as well as the regions spanning E-boxes in genes of interest.

Immune-system mediated liver damage: Age-matched adult mice were injected intravenously with Concanavalin A (Sigma-Aldrich) at 15 mg/kg or vehicle. Injections took place 24, 48, 72, 96, and 120 hr before tissue collection. All mice were culled simultaneously and their livers were collected and processed for flow-cytometry based BH3 Profiling as outlined above.

Supplemental References

Bauer, M., Cheng, S., Jain, M., Ngoy, S., Theodoropoulos, C., Trujillo, A., Lin, F.C., and Liao, R. (2011). Echocardiographic speckle-tracking based strain imaging for rapid cardiovascular phenotyping in mice. Circ. Res. *108*, 908–916.

Kaech, S., and Banker, G. (2006). Culturing hippocampal neurons. Nat. Protoc. *1*, 2406–2415.

Kim, M.-S., Pinto, S.M., Getnet, D., Nirujogi, R.S., Manda, S.S., Chaerkady, R., Madugundu, A.K., Kelkar, D.S., Isserlin, R., Jain, S., et al. (2014). A draft map of the human proteome. Nature *509*, 575–581.

Lindsten, T., Ross, a J., King, a, Zong, W.X., Rathmell, J.C., Shiels, H. a, Ulrich, E., Waymire, K.G., Mahar, P., Frauwirth, K., et al. (2000). The combined functions of proapoptotic Bcl-2 family members bak and bax are essential for normal development of multiple tissues. Mol. Cell *6*, 1389–1399.

Miller, J. a, Ding, S.-L., Sunkin, S.M., Smith, K. a, Ng, L., Szafer, A., Ebbert, A., Riley, Z.L., Royall, J.J., Aiona, K., et al. (2014). Transcriptional landscape of the prenatal human brain. Nature *508*, 199–206.

Minogue, A.M., Stubbs, A.K., Frigerio, C.S., Boland, B., Fadeeva, J. V, Tang, J., Selkoe,

D.J., and Walsh, D.M. (2009). gamma-secretase processing of APLP1 leads to the production of a p3-like peptide that does not aggregate and is not toxic to neurons. Brain Res. *1262*, 89–99.

Montero, J., Sarosiek, K.A., DeAngelo, J.D., Maertens, O., Ryan, J., Ercan, D., Piao, H., Horowitz, N.S., Berkowitz, R.S., Matulonis, U., et al. (2015). Drug-Induced Death Signaling Strategy Rapidly Predicts Cancer Response to Chemotherapy. Cell *160*, 977–989.

Ryan, J., and Letai, A. (2013). BH3 profiling in whole cells by fluorimeter or FACS. Methods.

Suzuki, M., Youle, R.J., and Tjandra, N. (2000). Structure of Bax: coregulation of dimer formation and intracellular localization. Cell *103*, 645–654.

Walsh, D.M., Thulin, E., Minogue, A.M., Gustavsson, N., Pang, E., Teplow, D.B., and Linse, S. (2009). A facile method for expression and purification of the Alzheimer's disease-associated amyloid beta-peptide. FEBS J. *276*, 1266–1281.

Zha, J. (2000). Posttranslational N-Myristoylation of BID as a Molecular Switch for Targeting Mitochondria and Apoptosis. Science (80-.). *290*, 1761–1765.